AGGREGATION OF HYDROPHOBIC COLLOIDS AND PROTEINS: SIZE DEPENDENT BEHAVIOR AND CROSSOVER TO INSTABILITY

Thesis Submitted in Partial Fulfillment of the Requirements for the Award of the Degree of

MASTERS OF SCIENCE
in
PHYSICS

Submitted by:

NEHA V. K.
(Roll No. 24/MSCPHY/60)

Under the supervision of
PROF. HIMADRI B. BOHIDAR
Honorary Faculty

DEPARTMENT OF APPLIED PHYSICS
DELHI TECHNOLOGICAL UNIVERSITY
(Formerly Delhi College of Engineering)
Bawana Road, Delhi – 110042

DEPARTMENT OF APPLIED PHYSICS

DELHI TECHNOLOGICAL UNIVERSITY

(FORMERLY DELHI COLLEGE OF ENGINEERING)

Bawana road, Delhi – 110042

CANDIDATE'S DECLARATION

I, **Neha V K**, Roll No. **24/MSCPHY/60**, hereby certify that the work being presented in the dissertation entitled **"Aggregation of Hydrophobic Colloids and Proteins: Size Dependent Behavior and Crossover to Instability"** in partial fulfillment of the requirements for the Degree of Master of Science, submitted to the Department of Applied Physics, Delhi Technological University, is an authentic record of my own work carried out under the supervision of **Prof. Himadri B Bohidar**. The matter presented in this dissertation has not been submitted by me for the award of any other degree, diploma, associateship, fellowship, or any other similar title or recognition. The work presented in this dissertation has been communicated to a reputed journal **Colloid and Polymer Science**, and part of the work has been presented as an oral presentation at the international conference **ICRANN – 2025**, with the following details:

Title of the paper 1: Aggregation of Hydrophobic Colloids and Proteins: Size Dependent Behavior and Crossover to Instability
Author names: Neha V K, Himadri B Bohidar
Journal Name: Colloid and Polymer Science
Status of paper: Manuscript has been submitted and is under processing.
Date of paper communication: 06.05.2026

Title of the paper 2: Hydrophobic Aggregation of Nanoparticles of Biological Origin

Author names: Neha V K, Himadri B Bohidar

Name of Conference: International Conference on Recent Advances in Nanoscience and Nanotechnology (ICRANN – 2025)

Conference date with venue: 20-21 December – 2025, Special Centre for Nanoscience (**SCNS**), Jawaharlal Nehru University, New Delhi

Registered for the Conference: Yes

Oral Presentation: Completed.

Place: Delhi

Date: 22.05.2026 NEHA V K

SUPERVISOR CERTIFICATE

I hereby certify that the Project Dissertation titled **"Aggregation of Hydrophobic Colloids and Proteins: Size Dependent Behavior and Crossover to Instability"** which is submitted by **NEHA V K**, Roll No(s). **24/MSCPHY/60** Department of Applied Physics, Delhi Technological University, Delhi in partial fulfillment of the requirement for the award of the degree of Master of Science, is a record of the project work carried out by the student under my supervision. To the best of my knowledge this work has not been submitted in part or full for any Degree or Diploma to this University or elsewhere.

Place: Delhi PROF. HIMADRI B. BOHIDAR

Date: 22.05.2026 Supervisor

ACKNOWLEDGEMENTS

I would like to express my sincere gratitude to my SUPERVISOR, **PROF. HIMADRI B. BOHIDAR**, Honorary Faculty, Department of Applied Physics, Delhi Technological University, for giving me the opportunity to work under his guidance. I am truly thankful to him for introducing me to the fascinating world of Biophysics and for being the best possible guide throughout this project. His deep knowledge, insightful suggestions, and continuous encouragement have been invaluable in shaping the present work. He has not only guided me in scientific research but also taught me to think critically, approach problems with clarity, and appreciate the bigger picture. His constant inspiration and support have greatly enriched this experience.

My sincere thanks to the Department of Applied Physics, Delhi Technological University, for the academic support and resources provided throughout this work.

I express my sincere gratitude to my mother, Veena P K, my father, T M Krishnakumar, and my sister, Niranjana V K, for their endless encouragement and support throughout this journey.

A special thanks to my colleague Amishi for her camaraderie and support during this work.

Lastly, I would like to fondly thank my dog, whose presence back home has always brought comfort and positivity, even from afar.

NEHA V K

AGGREGATION OF HYDROPHOBIC COLLOIDS AND PROTEINS: SIZE DEPENDENT BEHAVIOR AND CROSSOVER TO INSTABILITY

Neha V K

ABSTRACT

In this study, the aggregation properties of mainly hydrophobic proteins and colloids are explored by using an extended DLVO model that included an extra short-range interaction. Two different interaction regimes are studied to isolate the effect of hydrophobic interactions on protein aggregation. In the first interaction regime, van der Waals attraction, electrostatic double-layer repulsion, and short-range surface interactions are considered, and the interaction curves are described by finite energy barriers that kinetically stabilize protein dispersions over a broad size (R = 5-100 nm) and hydrophobicity (h_f = 0-20 %) range. In the second interaction regime, hydrophobic attraction is described by an exponential potential, causing the electrostatic barrier to collapse beyond a critical size, and resulting in a diffusion-limited, irreversible protein aggregation. The maximum interaction force (F_{max}) - size scaling analysis shows, $F_{max} \sim R^{\pm\alpha}$, with α = 0.5 for the first interaction regime, whereas in the second (hydrophobicity-dominated) interaction regime, this scaling linearly decreases with size (α = -0.5), indicating the lack of finite energy barriers and the dominance of short-range attraction. These results demonstrate that hydrophobic interactions by themselves are capable of inducing aggregation in electrostatically balanced systems. As a test, aggregation pattern in two predominantly hydrophobic proteins, elastin and zein, are discussed within the framework of Model-2 with satisfactory outcomes. Overall, this study clearly shows a size-dependent crossover from attraction-dominated behavior at small sizes to an unstable interaction regime at larger sizes, a conclusion that can be extended to colloidal, intrinsically disordered proteins and nanoparticle systems where surface hydrophobicity is profound.

Keywords: Hydrophobic protein aggregation, non-DLVO model, interaction potential, size-dependent crossover, interaction force-particle size scaling.

TABLE OF CONTENTS

LIST OF FIGURES

LIST OF TABLES

LIST OF ABBREVIATIONS & SYMBOLS

Abbreviation	Full Form
DLVO	Derjaguin–Landau–Verwey–Overbeek
IDPs	Intrinsically Disordered Proteins
LJ	Lennard–Jones
EDL	Electric Double Layer
DH	Debye–Hückel
vdW	van der Waals

Symbol	Meaning
R	Particle radius
r	Interparticle separation distance
r/R	Dimensionless separation distance
$U(r)$	Interaction potential
U_{LJ}	Lennard–Jones potential
U_{DL}	Double-layer interaction potential
U_{surf}	Surface interaction potential
U_{bar}	Energy barrier
U_{min}	Primary minimum interaction energy
F_{max}	Maximum interaction force
k_B	Boltzmann constant
T	Absolute temperature
k_BT	Thermal energy
k^{-1}	Debye screening length
λ_D	Debye length
λ_h	Hydrophobic decay length
λ_{surf}	Surface interaction decay length
A_h	Hydrophobic interaction amplitude
A_{DL}	Electrostatic interaction prefactor
C_{surf}	Surface interaction coefficient
σ	Molecular length scale
ϵ	Lennard–Jones energy parameter
r_0	Shift parameter
h_f	Hydrophobic fraction
k_BT	Thermal Energy
R_g	Radius of Gyration
R_h	Hydrodynamic Radius
F_{max}	Maximum Interaction Force

Chapter – 1

INTRODUCTION

1.1 BACKGROUND AND MOTIVATION

Self-assembly or aggregation of proteins is the most significant contributor to neurological and neurodegenerative pathogenic conditions like, the Alzheimer's, Parkinson's, Huntington, Amyotrophic Lateral Sclerosis, Creutzfeldt Jakob Dementia, Prion diseases, Amyloidosis and other forms of dementia. Proteinopathy is a recently coined term which refers to the conditions where proteins become structurally abnormal or fail to fold into stable secondary structures. This morphological change may contribute to the formation of oligomeric aggregates that adversely interfere with multiple biochemical processes leading to serious pathological consequences. Therefore, it is pertinent to develop a better understanding of this phenomenon.

Proteins are biopolymers composed of polar and non-polar amino acids arranged along a peptide backbone [1]. When dispersed in aqueous environment, the exposure of hydrophobic amino acid residues to water is energetically unfavourable that leads to their partial exclusion from the protein surface and the emergence of cooperative folding forces that reorganize the protein interior [2]. As a result, hydrophobic residues tend to cluster, forming compact structural motifs that stabilize native conformations while simultaneously influencing long-range intermolecular interactions. This hydrophobic driving force plays a central role in protein self-assembly, misfolding, and aggregation phenomena [2,3]. There exist a class of proteins that are structurally disordered (intrinsically disordered proteins, IDPs), and proteins comprising of large amount of hydrophobic amino acids (like leucine, isoleucine, valine, phenylalanine, and methionine) that exhibit aggregation behavior not accountable by DLVO type description [4]. Some examples of IDPs are p27, p53, CREB α-synuclein, tau, elastin, CREB, amyloidogenic proteins etc. These proteins are characterised by their short-range folding complexity and unusual aggregation tendency. Among the hydrophobic proteins elastin, zein, prolamin, silk fibroin and transmembrane proteins are biologically relevant [5,6]. Therefore, understanding the interaction mechanisms that lead to the aggregation pattern of these predominantly hydrophobic biomolecules is necessary, furthermore such a model must account for the degree of hydrophobicity, and size of the biomolecules among other parameters.

From a physical standpoint, proteins in solution may be viewed as complex colloidal particles whose stability is governed by the balance between attractive and repulsive intermolecular forces [7]. The classical Derjaguin-Landau-Verwey-Overbeek (DLVO) theory is a fundamental theoretical basis for understanding such interactions, taking into consideration the competition between the van der Waals attraction and the electrostatic repulsive forces due to the overlap of the electric double layers [8] . The interaction potential usually has a strong primary minimum at short range, a finite repulsive energy barrier at intermediate range, and a shallow secondary minimum at long range [9]. Aggregation takes place when the attractive forces prevail or when the electrostatic barrier is sufficiently lowered, allowing access to the primary minimum [10]. Salt-mediated aggregation of colloids and proteins is a result of DLVO-type interactions [8,11-13].

A stable dispersion of biomolecules in water requires its proper hydration by the creation of successive hydration layers around its surface [14]. In the case of biomolecules with high hydrophobicity, such hydration becomes problematic, and therefore the stability of their dispersion must be considered properly by taking into consideration their hydrophobicity [15]. Hydrophobic proteins, in particular, owing to their special amino acid composition, are problematic in terms of traversing their free-energy landscape of dispersion stability in water [16].

In this prominent biopolymer category, the presence of non-polar side chains promotes hydrophobic interactions and affects the interfacial water structure, thus deviating from the predicted balance according to classical DLVO theory [3]. In aqueous solution, hydrogen bonding between biomolecular functional groups and water molecules is a fundamental mechanism in the stabilization of biomolecular structures, whereas hydration layers and solvent structuring effects introduce new short-range forces that are not accounted for in the classical DLVO theory [17]. At the molecular level, binding attraction forces can be modelled using Lennard-Jones or Morse potentials, which are versatile models of short-range binding forces in biomolecular association [18].

Therefore, a complete understanding of hydrophobic protein/colloid aggregation must necessarily incorporate the interaction model with non-DLVO contributions such as hydrophobic forces and surface-specific forces [8]. These extended DLVO models, based on colloid and polymer physics, provide a physically consistent framework for understanding the potential impact of hydrophobic regions on interaction forces and the aggregation of proteins into larger, typically biologically inactive entities [2,3,8].

1.2 HIGHLIGHTS

- Hydrophobic proteins/colloids undergo distinctive aggregation.
- Hydrophobic and surface forces must be included in the DLVO theory to address this issue.
- The extended DLVO formulation revealed universal scaling of maximum interaction force with size.
- Under dominating hydrophobic interactions, a size and hydrophobicity dependent crossover to instability was noticed.

Chapter – 2

THEORY AND LITERATURE REVIEW

The evolution of polymer science established the conceptual foundation required for understanding biological macromolecules. Early development by Staudinger introduced the macromolecular perspective, and subsequent contributions by Flory laid the statistical interpretation of long-chain systems, which are presently applied for describing biopolymeric assemblies such as proteins and nucleic acids [1]. These theoretical frameworks enable biological macromolecules to be treated as polymeric chains, where the chain architecture and monomer connectivity determine higher-order structural properties [1]. From a microscopic viewpoint, a polymer consists of repeating monomeric units whose total molecular mass may be expressed in terms of the monomer mass.

$$M_{poly} = N \, x \, M_{monomer} \qquad (1.0)$$

Parameters such as monomer functionality govern whether linear, branched, or more complex network structures are formed [1]. Several classifications such as homopolymers, copolymers and block copolymers are commonly used in synthetic polymer studies naturally extend to biopolymers, providing a physical interpretation of structural complexity.

Interaction Forces Relevant for Biomacromolecules

The structure of biomolecules involves both covalent and non-covalent bonding. The latter includes interactions such as electrostatic forces, hydrogen bonding, excluded-volume interactions, van der Waals attractions and hydrophobic forces [1], [3–5]. Because of interactions between oxygen and nitrogen atoms, hydrogen bonds predominate in aqueous biological settings, while van der Waals attractions, which are weak on their own, become significant because of their cumulative influence across extended molecule surfaces (Table 1).

Table 1: Typical energies and bond lengths for primary covalent bonds and major secondary intermolecular forces.

Secondary Forces	Energy (kcal/mol)	Bond length (Å)	Notes
Covalent Bond	50-120 (avg.~ 83)	1.0-2.0 (avg.~1.5)	Strongest Chemical bond, defines molecular connectivity
Electrostatic interaction	5-20	2.8-3.5	Strongest non-covalent force
Hydrogen bonding	3-10	1.5-2.5	Directional, key in biomolecular folding
Excluded volume interactions	repulsive	<2	Very short range, prevents overlap
Vander waal forces	0.5-1 (per pair)	3.5-4.0	Weak, cumulative effect important

Hydrophobic forces emerge due to the exclusion of non-polar groups from water and represent an entropically driven process that strongly influences protein folding and aggregation [2], [5].

Hydrogen bonding between water molecules and biomolecular groups plays a crucial role in stabilizing folded structures in solution, and the spatial extent and energetic strength of these interactions generate both attractive and repulsive contributions that ultimately regulate biomolecular association.

Polymer Conformation and Characteristic Length Scales

Characteristic statistical length metrics including the end-to-end distance, radius of gyration R_g, hydrodynamic radius R_h, persistence length, and contour length are widely used in polymer physics [1]. The radius of gyration, which is often obtained by scattering techniques, quantifies the average distribution of monomeric mass with respect to the center of mass of the polymer.

$$\overrightarrow{R_g^2} = \frac{1}{N^2}\sum_{i,j=1}^{N}\langle(\overrightarrow{R_i} - \overrightarrow{R_j})^2\rangle \qquad (1.1)$$

Similarly, R_h describes the diffusion-derived hydrodynamic size of a macromolecule in solution.

$$R_h = \frac{K_B T}{6\pi\eta D} \qquad (1.2)$$

The conformational ratio R_g/R_h is sensitive to chain flexibility and solvent quality and assumes characteristic values for different geometric structures *(Table 2)*.

Table 2: Characteristic values of the conformational ratio R_g/R_h for different molecular shapes and their physical significance.

Conformation / Shape	R_g/R_h	Significance
Hard sphere	~0.775	Dense, spherical object
Flexible random coil (ideal chain)	~1.50 – 1.78	Unperturbed chain in theta solvent; follows Gaussian statistics
Self – avoiding walk (good solvent)	~1.55 – 1.65	Swollen coil due to excluded volume
Rod – like chain	~1.73 – 2.00	Highly extended conformation; large R_g due to long shape, small R_h
Dumbbell	~1.0 – 1.2	Intermediate shape between sphere and coil
Star polymer (branched)	<1.5	Branched coil; smaller R_g due to compact branching

Persistence length is used to quantify chain stiffness and may combine intrinsic stiffness with electrostatic contributions in charged systems.

Charge Effects: Polyelectrolytes and Polyampholytes

Polyelectrolytes are biopolymers with ionizable groups, while polyampholytes are proteins with both basic and acidic residues [1]. Their effective charge fluctuates significantly with pH, resulting in an isoelectric point where the net charge disappears. Hydrodynamic behavior, electrostatic interactions, electrophoretic mobility, and aggregation tendency are all directly impacted by this charge sensitivity. Osmotic pressure changes and counterion condensation, which are common in polyelectrolyte solutions, also occur in protein systems and provide a theoretical connection between biomolecular interactions and polymer physics. Because these electrostatic effects alter both attractive and repulsive force components, they are essential in determining colloidal stability [1], [4].

Electrostatic Screening and Debye–Hückel Framework

Electrostatic interactions are strongly modulated by ionic environments. Debye–Hückel theory explains that mobile ions rearrange around a charged biomolecule, resulting in exponential decay of electrostatic potential with distance characterized by a Debye screening length κ^{-1} [4].

$$\boldsymbol{k = \left(\frac{8\pi N_A \epsilon^2}{1000 D k_B T}\right)^{\frac{1}{2}} . I^{\frac{1}{2}}} \qquad \textbf{(1.3)}$$

Table 3: A relationship between ionic strength and screening length

Ionic Strength (M)	Screening Length (κ^{-1}) (nm)
0.001	9.58
0.01	3.03
0.1	0.96
0.5	0.43
1	0.30

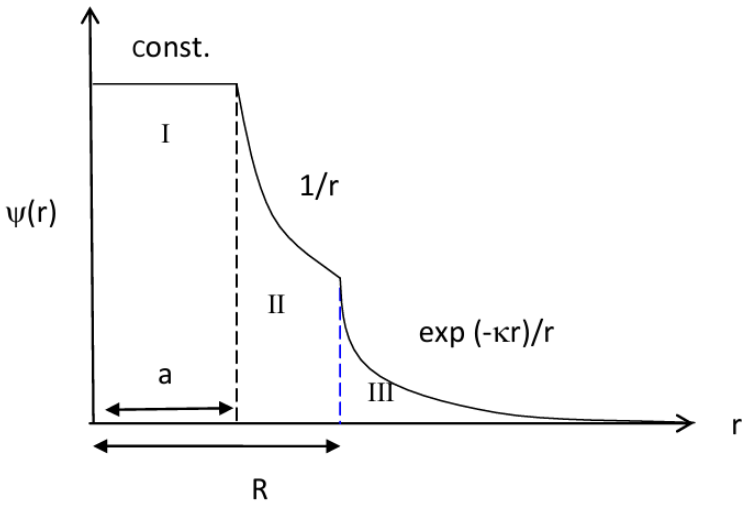

Fig. 1 Depiction of potential ψ(r) around the spherical macroion

In the Stern layer, the potential falls rapidly as reciprocal of distance. In the diffuse layer, the potential decays exponentially with a characteristic decay length κ^{-1} called the Debye screening length.

(i) Region I: no mobile ions; Laplace equation is valid

(ii) Region II: no mobile ions; Laplace equation is valid

(iii)Region III: mobile ions; Poisson equation is valid

$$\text{I. } \psi_I(\mathrm{r}) = \frac{q}{DR}\left(1 - \frac{kR}{1+ka}\right) : macroion\ core \qquad \textbf{(1.4)}$$

$$\text{II. } \psi_{II}(\mathrm{r}) = \frac{q}{Dr}\left(1 - \frac{kr}{1+ka}\right) : Stern\ layer \qquad \textbf{(1.5)}$$

$$\text{III. } \psi_{III}(\mathrm{r}) = \frac{q}{D}\left(\frac{e^{ka}}{1+ka}\right)\left(\frac{e^{-kr}}{r}\right) : Diffuse\ layer \qquad \textbf{(1.6)}$$

Increasing ionic strength shortens κ^{-1} and thereby diminishes long-range repulsion, offering a mechanistic route through which attractive forces may gain dominance in hydrophobic protein systems [2], [4]. These electrostatic considerations become essential when connecting colloid models to biological macromolecules.

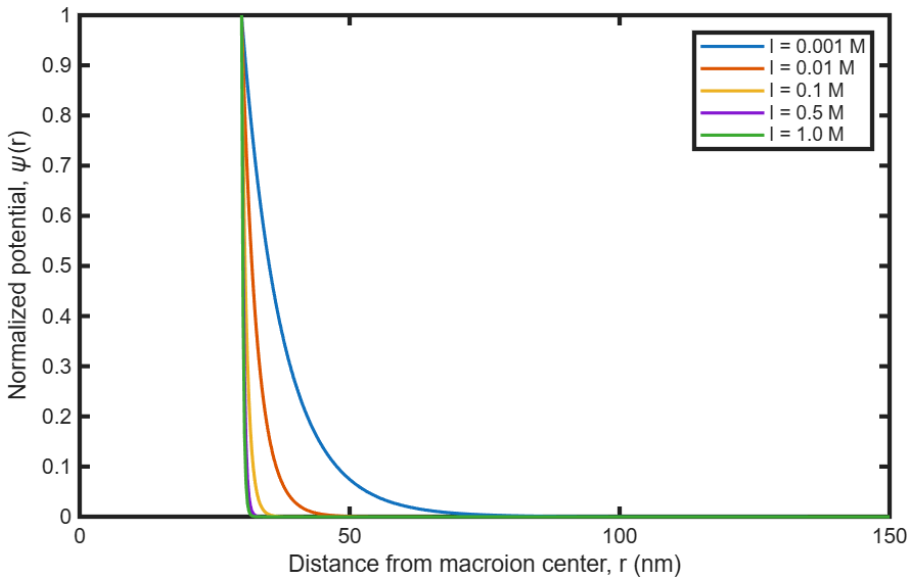

Fig. 2 Debye–Hückel Potential Profile for a Macroion at Different Ionic Strengths

Proteins: Structure, Folding, and Aggregation

Proteins consist of sequences of amino acids that establish hierarchical structural organization: primary (sequence), secondary (helices and sheets), tertiary (three-dimensional folding), and quaternary (multimeric association) [1].

Protein folding corresponds to a free-energy minimization process where hydrophobic collapse, hydrogen bonding, and electrostatic stabilization cooperatively lead to a thermodynamically favourable conformation [1], [2], [5]. Misfolding or partial unfolding may generate aggregation pathways that culminate in biologically inactive assemblies, which are associated with neurodegenerative and structural disorders. The physical mechanisms underlying such aggregation require analysis of both entropic and energetic contributions.

Polymerization Routes and Helical Growth

Viewed from a polymer-growth perspective, proteins arise through linear polymerization of amino acids via peptide bonding followed by conformational reorganization into ordered structures [1].

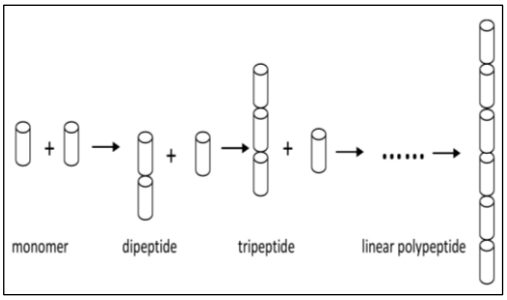

Fig. 3 Addition polymerization and growth of linear polypeptide molecule

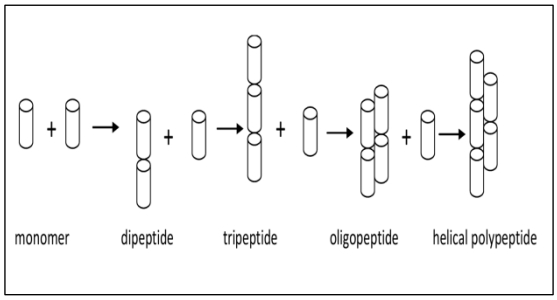

Fig. 4 Addition polymerization and growth of helical polypeptide molecule

Under favourable conditions, cooperative interactions promote helical growth, stabilised by intramolecular hydrogen bonding, leading to the emergence of well-defined secondary motifs [1], [5]. Linear and helical growth models provide a simplified physical interpretation of how local ordering emerges even in initially flexible chains.

Chapter – 3

DLVO FORCES

The classical Derjaguin–Landau–Verwey–Overbeek (DLVO) framework is widely employed to describe the net interaction energy between colloidal entities or surfaces dispersed in an aqueous environment. Within this approach, the measurable interaction potential originates from a competition between two dominant contributions namely, the universal van der Waals attraction and the electrostatic repulsion created by overlapping electric double layers [4]. Hence, the total interaction energy V_T can be expressed as the sum of attractive and repulsive terms (Equation 1.7), where the separation distance is denoted by h [4].

$$\boldsymbol{V_T = V_{vdW} + V_{EDL}} \qquad \textbf{(1.7)}$$

Attractive Van der Waals Contribution

Attractive interactions emerging from fluctuating dipoles (which include Keesom, Debye and London components) act universally in condensed matter systems and generally promote closer approach of particles or surfaces [4]. The magnitude and spatial decay of these forces depend strongly on geometry: molecular pairs typically scale as $1/d^6$, whereas planar, spherical or molecule - surface configurations show different distance dependencies.

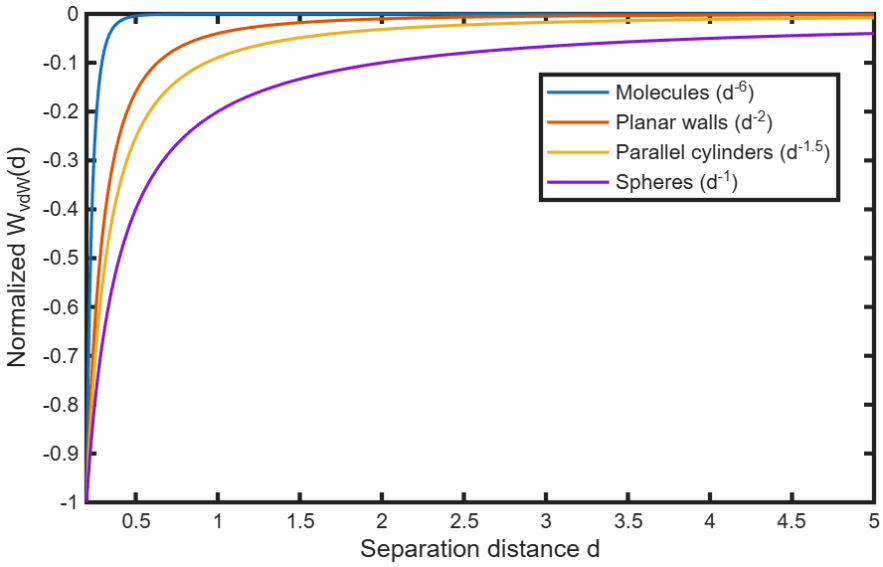

Fig. 5 Distance dependence of the van der Waals interaction for different geometries, showing that the interaction decays most rapidly for molecules and most slowly for spherical particles.

The dielectric characteristics of the interacting entities and the surrounding medium directly affect the Hamaker constant, which establishes the van der Waals term's strength. The interaction may even turn repulsive when the medium's optical characteristics fall between those of the two surfaces [4].

Repulsive Electric Double-Layer Contribution

A compact Stern area and an extended diffuse region make up the structured counterions distribution that charged interfaces form when submerged in electrolyte solution [4]. Overlap of these diffuse layers creates an osmotic pressure as two charged surfaces approach, balancing the attracting component and creating an effective barrier. The Debye screening length κ^{-1}, which decreases with increasing ionic strength, is used to quantify the typical thickness of this diffuse zone [4]. (Equation 1.3)

Shape of the DLVO Potential

Three unique regions may be seen in a traditional DLVO energy curve: a shallow secondary minimum at relatively greater separations, a finite repulsive energy barrier at intermediate distances, and a deep attractive minimum at very small separations (primary minimum) [4]. While moving past the barrier into the primary minimum causes persistent aggregation, staying in the secondary minimum is typically reversible. Changes in pH, electrolyte concentration, or surface charge density alter the barrier height and, as a result, control the likelihood of aggregation. A schematic DLVO curve that shows these characteristics can be observed in Fig.6.

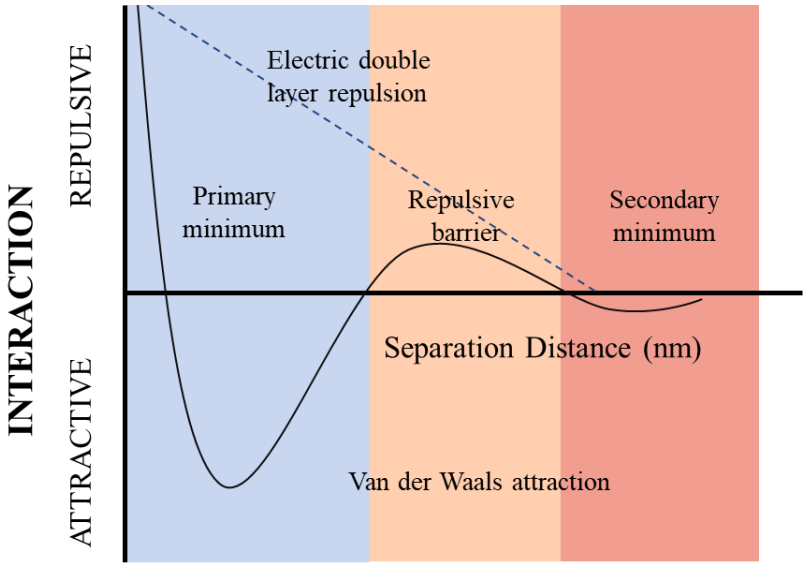

Fig. 6 Classical DLVO Curve

Colloidal Stability

Whether dispersion remains stable or undergoes aggregation depends upon the relative magnitude of the repulsive and attractive contributions. Increased ionic strength compresses the double layer, decreases the electrostatic barrier and therefore accelerates aggregation phenomena. Similarly, pH variations can alter surface charge states and move the system from a stable region to a coagulated state. These mechanisms are directly relevant to biological macromolecules in aqueous solution where screening of electrostatic interactions significantly affects aggregation behavior [2], [4].

Beyond Classical DLVO

Although DLVO analysis captures the essential balance between dispersion forces and double-layer repulsion, additional short-range forces may arise that are not included in the original formulation. Examples include hydrophobic interactions, hydration forces, steric repulsion due to polymers, ion – pair interaction in the presence of multivalent ions, and fluctuation forces in soft matter systems [2], [4], [5]. These non-DLVO interactions are particularly relevant for proteins due to their heterogeneous charge distribution and hydrophobic character, motivating modified DLVO treatments in protein aggregation studies [2], [4], [5].

Chapter – 4

MODIFIED DLVO THEORY

In order to evaluate the combined influence of attractive, electrostatic and surface-specific forces, numerical interaction profiles were generated by superposing three potential components. The calculations are based on dimensionless coordinates *r/R* and $U(r)/k_BT$, where R denotes an effective particle size and k_BT is the thermal energy at temperature T and U(r) is the interparticle interaction potential. This representation permits comparison across different sizes and surface fractions without altering the underlying functional forms [3,23].

(a) Model – 1

The first model employs a Lennard-Jones term for short-range molecular attraction $\mathbf{U_{LJ}}$, together with the Debye-Hückel electrostatic double-layer potential $\mathbf{U_{DL}}$ and a surface exponential term $\mathbf{U_{surf}}$ describing hydrophobic or hydration forces given by

$$U_{total} = U_{LJ} + U_{DL} + U_{surf} \qquad \textbf{(2)}$$

Lennard–Jones potential $\mathbf{U_{LJ}}$ captures hard-core exclusion at very short separations followed by an attractive tail consistent with molecular pair interactions [24] given by

$$U_{LJ}(r) = 4\varepsilon\left[\left(\frac{\sigma}{r+\sigma_0}\right)^{12} - \left(\frac{\sigma}{r+\sigma_0}\right)^{6}\right] \qquad \textbf{(3)}$$

σ is the molecular length and ε defines the strength of the potential. σ_0 is the small shift to avoid singularity at *r=0*. This potential comprises of a very short-range repulsion $(\propto r^{-12})$ plus long-range attraction $(\propto r^{-6})$.

Double Layer interaction is a repulsive interaction decaying with a screening length κ^{-1} (Debye length) is given by [25]

$$U_{DL}(r) = A_{DL}\frac{a}{a+r}e^{-kr} \qquad \textbf{(4)}$$

A_{DL} is a constant set by surface potential/ionic strength.

The additional potential term U_{surf} is taken as a phenomenological term parameterised by the magnitude C_{surf} and decay length λ_{surf} representing hydrophobic attraction structuring is given by

$$U_{surf}(r) = C_{surf}ae^{-r/\lambda_{surf}} \qquad \textbf{(5)}$$

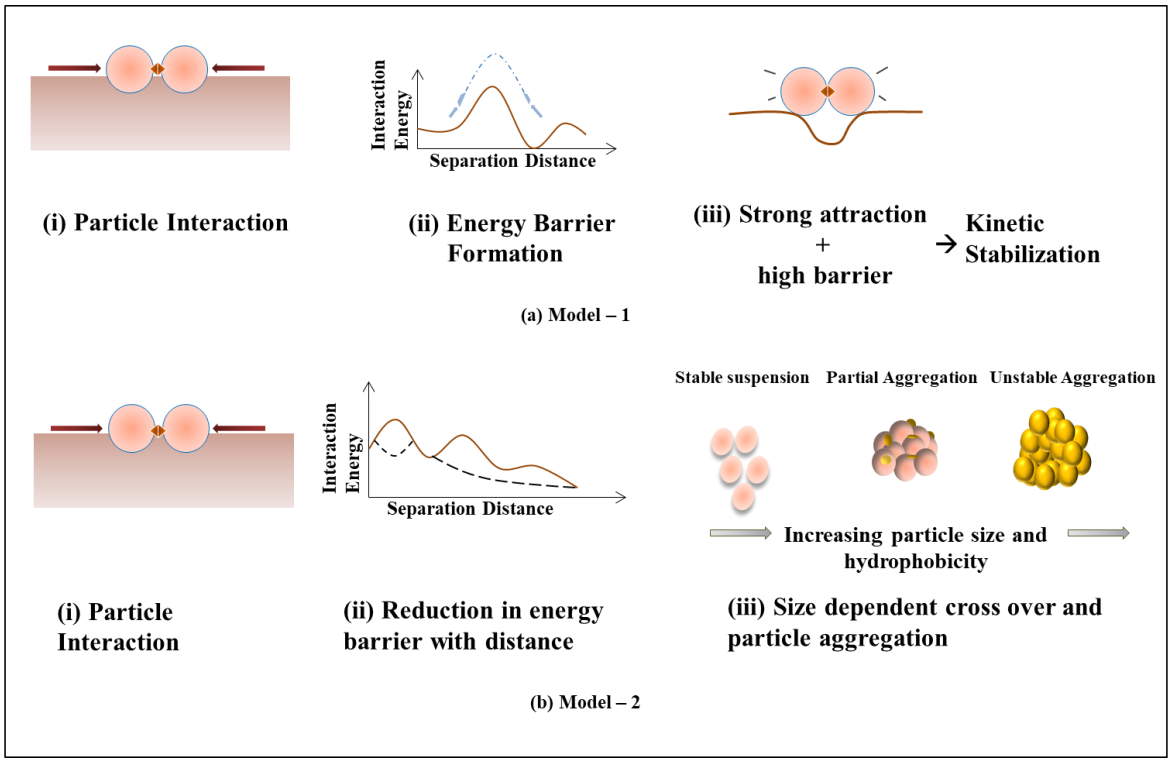

Fig. 7 Interaction landscapes for the two interaction models. (a) Model-1 has a deep primary minimum separated by a finite energy barrier due to a balance of short-range Lennard-Jones attraction and electrostatic repulsion, leading to kinetically stable dispersions. (b) Model-2 illustrates the aggregation phenomenon caused by hydrophobicity, where increasing particle size and hydrophobicity continue to decrease the energy barrier until it collapses, leading to a transition from a stable dispersion to an aggregation state.

(b)Model – 2

The second model replaces the Lennard-Jones attraction with a tunable hydrophobic exponential potential (Eq. 6), thereby isolating the effect of hydrophobic forces without invoking a strong hard-core repulsion. This potential is given by

$$U_{hydro}(r) = -A_h \frac{a}{a+r} e^{-r/\lambda_h} \qquad (6)$$

Where A_h controls the amplitude and λ_h sets the range of this potential [15]. This potential is characterized by a short-range interaction (attraction) with sufficient tunability to produce deeper primary minimum without adding hard-core repulsion

The two models are logically constructed to distinguish kinetically stabilized interaction landscapes to smoothly navigate from the hydrophobicity-dominated aggregation regimes. This way of formulation enables the depth of the primary well to be varied independently by changing the hydrophobic amplitude and range. In this case, aggregation can be initiated without necessarily lowering the electrostatic barrier, as seen in hydrophobic protein systems [26].

4.1 Choice of Model Parameters

All computations were carried out using the same set of numerical bias and interaction parameters, and the alterations were only included when specifically mentioned, to enable a controlled comparison between the two interaction models. A hydrophobic surface fraction of $h_f = 10\%$ (degree of hydrophobicity) was selected as the foundation for additional investigation in the structured analysis. With a finite electrostatic energy barrier, this modest to moderate degree of hydrophobicity is adequate to affect near-contact interactions. Since both models used the same hydrophobic fraction, any variations in interaction behavior can only be attributed to the attractive interaction's contribution.

4.1.1 Baseline Interaction Parameters

A Lennard-Jones potential was used in Model-1 to simulate the short-range attraction. The molecule length scale was chosen at $\sigma = 0.35\ nm$ and the energy scale at $\varepsilon = 20k_BT$. A small shift parameter, $r_0 = 0.05\ nm$, was used to provide numerical stability at contact and prevent divergence when particles get too close. Both models employed the Debye-Huckel form for the electrostatic repulsion. The Debye length was $\lambda_D = \kappa^{-1} = 0.8\ nm$, and the prefactor was $A_{DH} = 30\ k_BT$. To ensure the same electrostatic bias in every simulation, these variables were maintained constant. A short-range surface interaction with a decay length of λsurf = 6 nm and an amplitude of $C_{surf} = 3\ k_BT\ nm^{-1}$ was incorporated. When necessary, this section was modified depending on the hydrophobic surface fraction (h_f) to account for additional effects close to the surface.

4.1.2 Hydrophobic Interaction Parameters

Model-2 was created with hydrophobic attraction explicitly included by an exponential interaction with a decay length of $\lambda_h = 0.35\ nm$ and a strength of $A_h = 80\ k_BT$. These characteristics allowed for a direct comparison with the Lennard-Jones attraction utilized in Model-1 while modeling strong and short-range hydrophobic interactions pertinent to biomolecular and colloidal systems.

4.1.3 Particle Size and hydrophobicity dependence

The baseline interaction regimes and stability were analyzed using a fixed particle size of $a = 5nm$. The separation between particles was presented in terms of the non-dimensional distance r/R, with R being the effective size of the particle.

In order to study how hydrophobicity affects the interactions potentials and stability, hydrophobic fractions $h_f = 0\%, 5\%, 10\%, 15\%$ and 20% were considered in each model. Both models were examined for the set sizes of $R = 5, 25, 50, 75,$ and $100\ nm$, thus allowing us to investigate how changes in surfaces and sizes affect the interactions between particles. Interaction regimes were classified depending on the energy barrier that separates regions of attraction and repulsion: (i) stable regime ($U_{bar} > 10\ k_BT$), (ii) metastable regime ($1 < U_{bar} \leq 10\ k_BT$), and (iii) unstable regime ($U_{bar} \leq 1\ k_BT$). This classification provides a consistent framework in comparing kinetic stability for various models and parameter sets. Furthermore, it will be appropriate to place the energy scales discussed above in the right perspective *vis a vis* protein aggregation. At the room temperature (300 K), the thermal energy k_BT is close to the hydrogen bond energy (i.e. few kcal/mol). Often the aggregation in biopolymers, and the proteins in particular, is due to the formation of intermolecular hydrogen bonds [27]. Thus, the energy requirement for the stability defined above (10 k_BT) is equivalent to saying any aggregate with at least ~10 H-bond contacts is rigid and stable. The intermolecular interactions play a key role in bringing individual molecules closer. Then, the secondary forces get activated and aggregation ensues. In the discussion that follows, the models predict the energy barrier that must be overcome to establish aggregation.

All interaction energies were normalized by the thermal energy scale k_BT, and results are presented using the reduced interaction potential U/k_BT and the dimensionless separation r/R. Interaction forces were obtained from the first derivative of the interaction potential with respect to separation. The maximum attractive force was extracted for each particle size, and a linear fitting was performed between the maximum interaction force F_{max} and particle size R to quantify size-dependent force scaling under fixed hydrophobic and electrostatic conditions.

Chapter – 5

SIMULATION RESULTS AND DISCUSSIONS

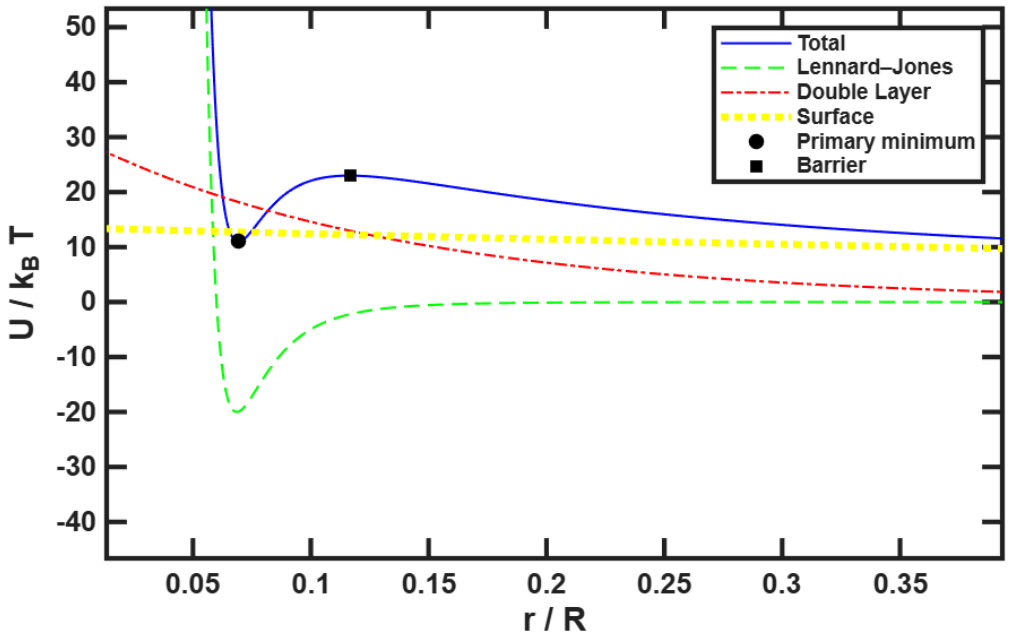

Fig. 8 Model-1 interaction potential for 10% hydrophobicity at R=5 nm, showing Lennard–Jones attraction, electric double-layer repulsion and surface contributions with a clearly resolved primary minimum and barrier.

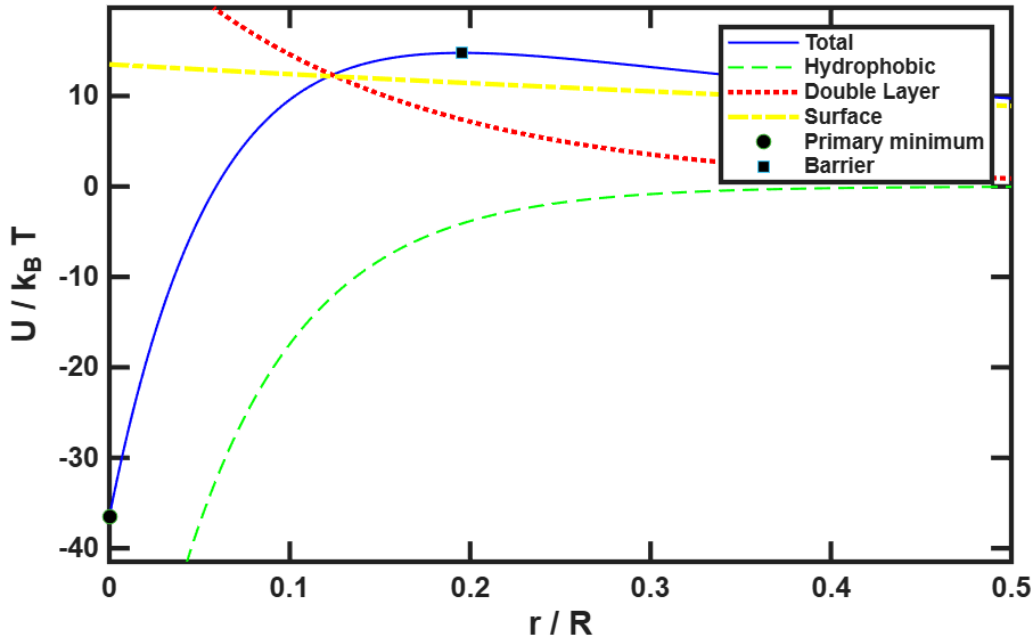

Fig. 9 Model-2 interaction potential for 10% hydrophobicity at R=5 nm, demonstrating a deep hydrophobic well and a finite electrostatic barrier in the short-range molecular regime.

The two interaction models yield qualitatively different short-range interaction landscapes at 10% hydrophobicity and particle size R=5 nm. A stable interaction profile

with a finite primary minimum separated from contact by an energy barrier was noticed in Model-1. This can be interpreted as the combined effects of Lennard–Jones attraction, electrostatic repulsion, and surface interactions. In contrast, Model-2 exhibits a strongly attractive short range interaction dominated by a hydrophobic exponential potential. Although an electrostatic contribution is present, the overall interaction profile doesn't display a pronounced stabilizing barrier separating the primary minimum from particle contact. The depth of the attractive well in Model-2 is substantially greater than that of model-1 under identical biases. The detailed contributions of the each interaction terms and the resulting potential profiles can be observed in Figs. 8 and 9.

5.1 Effect of Hydrophobicity on Interaction Potentials

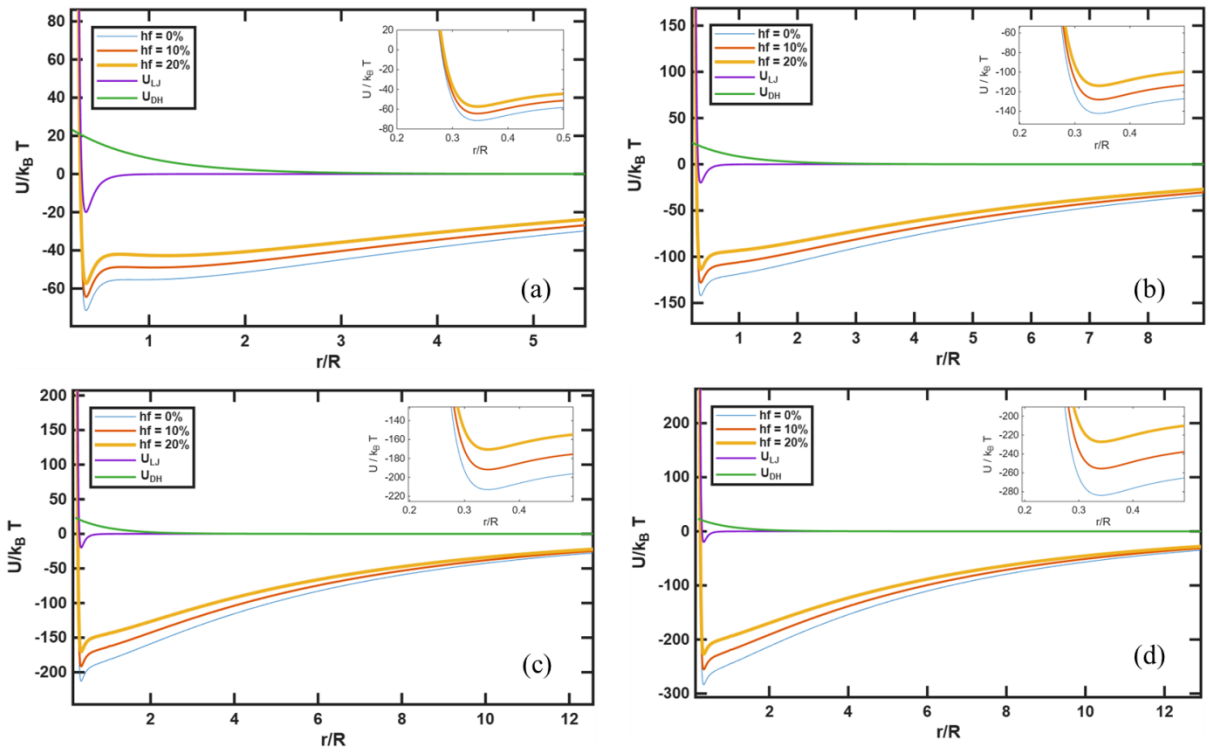

Fig. 10 Hydrophobicity dependence of the interparticle interaction potential in Model – 1 for increasing particle size: (a) a=25 nm, (b) a=50 nm, (c) a=75 nm, and (d) a=100 nm.

Figure 10 demonstrates the influence of the hydrophobicity on the dependence of the interaction potential for Model-1 particles of different sizes. The total interaction potential is generated by the balance between the short-range attractive and long-range electrostatic repulsive contributions.

As the hydrophobicity grows, regardless of the particle size the depth of the primary minimum increases, which means that the stronger interaction occurs for more hydrophobic surfaces. At the same time, the location of the primary minimum almost does not change for all sizes and stays at the value $r_{min} \approx 0.34$; see inset graphs for the range of r = 0.2 – 0.5 nm.

The inset focuses on the region close to the point of contact, where both the minimum and the energy barrier exist. As the depth of the primary minimum depends on the hydrophobicity, the barrier is weakly dependent on it for small-sized particles; however, due to a relatively high energy barrier, it still guarantees kinetic stability.
The numerical data on U_{min}, r_{min}, and U_{bar} for different sizes of Model-1 particles along with corresponding stability regions are presented in Tables 4-7.

When a = 25 nm, the energy barrier is still large enough ($U_{bar} > 10\ k_BT$) at all hydrophobicities, creating a stable phase that corresponds to the repulsive barrier present in Fig. 10(a). However, with the growth of the particle size up to a = 50 – 100 nm, the barrier value becomes smaller, leading to an unstable phase in spite of the deep primary minimum. This implies that there is a shift from kinetic stabilization to irreversible aggregation with strong short-range attraction being dominant.

Table 4: Hydrophobicity dependence of interaction minimum, barrier height, and stability regime for Model-1 at R = 25 nm.

h_f (%)	U_{min}/k_BT	r_{min}(nm)	U_{bar}/k_BT	Regime
0	-71.51	0.34	16.18	Stable
5	-67.97	0.34	15.94	Stable
10	-64.43	0.34	15.72	Stable
15	-60.89	0.34	15.51	Stable
20	-57.35	0.34	15.31	Stable

Table 5: Hydrophobicity dependence of interaction minimum, barrier height, and stability regime for Model-1 at R = 50 nm.

h_f (%)	U_{min}/k_BT	r/R	U_{bar}/k_BT	Regime
0	-142.20	0.34	0.00	Unstable
5	-135.12	0.34	0.00	Unstable
10	-128.04	0.34	0.00	Unstable
15	-120.96	0.34	0.00	Unstable
20	-113.87	0.34	0.00	Unstable

Table 6: Hydrophobicity dependence of interaction minimum, barrier height, and stability regime for Model-1 at R = 75 nm.

h_f (%)	U_{min}/k_BT	r/R	U_{bar}/k_BT	Regime
0	-213.00	0.34	0.00	Unstable
5	-202.37	0.34	0.00	Unstable
10	-191.74	0.34	0.00	Unstable
15	-181.12	0.34	0.00	Unstable
20	-170.49	0.34	0.00	Unstable

Table 7: Hydrophobicity dependence of interaction minimum, barrier height, and stability regime for Model-1 at R = 100 nm.

h_f (%)	U_{min}/k_BT	r/R	U_{bar}/k_BT	Regime
0	-282.83	0.34	0.00	Unstable
5	-269.66	0.34	0.00	Unstable
10	-255.48	0.34	0.00	Unstable
15	-241.31	0.34	0.00	Unstable
20	-227.14	0.34	0.00	Unstable

Figure 11 illustrates the variation of the interaction potential energy as a function of the hydrophobic parameter in Model-2, when the particle sizes vary. As mentioned before, here the surface interaction is repulsive, hence, leading to a different form of interaction curve compared to Model-1.

It can be seen that the total interaction potential always stays **repulsive at short distances** and decreases monotonically with increasing distance. The **higher hydrophobicity** results in a **reduction in the strength of the interactions**, as shown by

the downward shifting of the interaction energy curves with the increase in the fraction of hydrophobic parameter. The same is also confirmed from the inset figures, which focus specifically on the region of contact (0.2-0.5 nm). The inset figures reveal that contrary to Model-1, no attractive minimum appears in the potential curve, irrespective of the value of hydrophobic parameter or the size of particles.

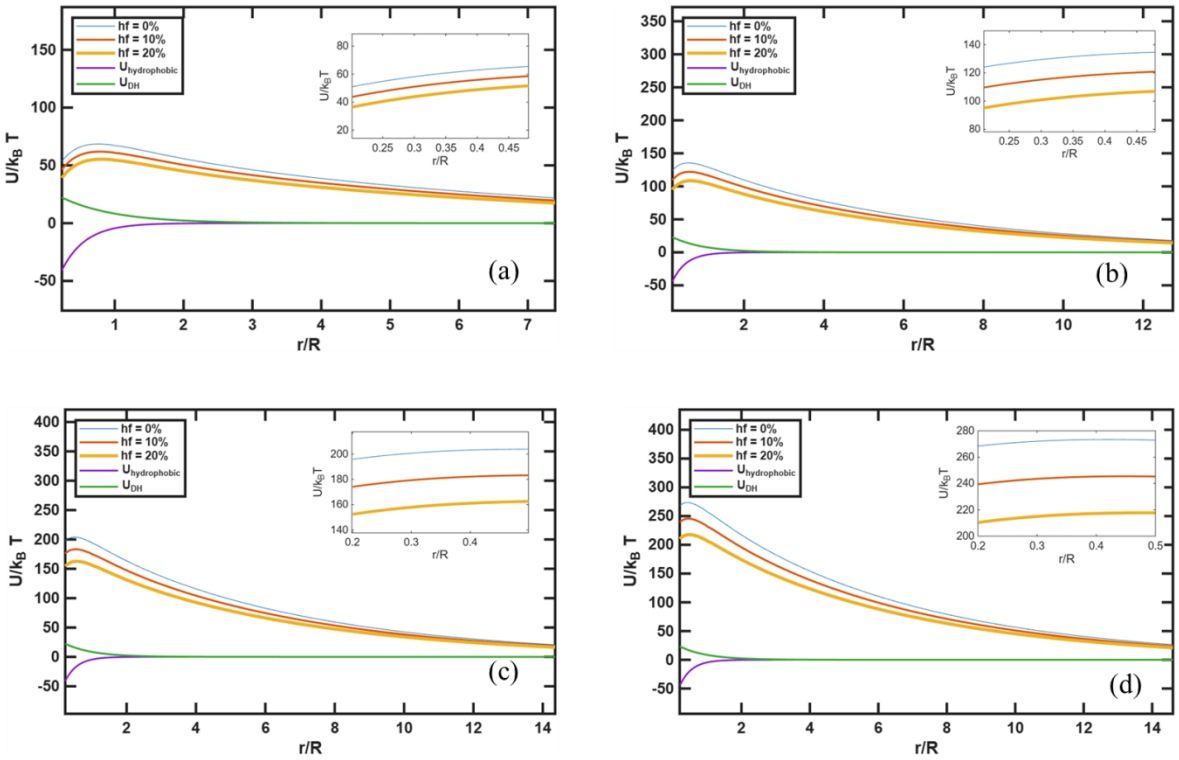

Fig. 11 Hydrophobicity dependence of the interparticle interaction potential in Model – 2 for increasing particle size: (a) a=25 nm, (b) a=50 nm, (c) a=75 nm, and (d) a=100 nm.

Table 8: Hydrophobicity dependence of interaction minimum, barrier height, and stability regime for Model-2 at R = 25 nm.

h_f (%)	U_{min}/k_BT	r/R	U_{bar}/k_BT	Regime
0	1.17	25.00	0.00	Unstable
5	1.12	25.00	0.00	Unstable
10	1.06	25.00	0.00	Unstable
15	1.00	25.00	0.00	Unstable
20	0.94	0.00	0.00	Unstable

Table 9: Hydrophobicity dependence of interaction minimum, barrier height, and stability regime for Model-2 at R = 50 nm.

h_f (%)	U_{min}/k_BT	r/R	U_{bar}/k_BT	Regime
0	2.35	25.00	0.00	Unstable
5	2.23	25.00	0.00	Unstable
10	2.11	25.00	0.00	Unstable
15	2.00	25.00	0.00	Unstable
20	1.88	25.00	0.00	Unstable

Table 10: Hydrophobicity dependence of interaction minimum, barrier height, and stability regime for Model-2 at R = 75 nm.

h_f (%)	U_{min}/k_BT	r/R	U_{bar}/k_BT	Regime
0	3.52	25.00	0.00	Unstable
5	3.35	25.00	0.00	Unstable
10	3.17	25.00	0.00	Unstable
15	2.99	25.00	0.00	Unstable
20	2.82	25.00	0.00	Unstable

Table 11: Hydrophobicity dependence of interaction minimum, barrier height, and stability regime for Model-2 at R = 100 nm.

h_f (%)	U_{min}/k_BT	r/R	U_{bar}/k_BT	Regime
0	4.70	25.00	0.00	Unstable
5	4.46	25.00	0.00	Unstable
10	4.23	25.00	0.00	Unstable
15	3.99	25.00	0.00	Unstable
20	3.76	25.00	0.00	Unstable

The lack of energy barrier in Model-2 directly affects the kinetics of aggregation processes. In absence of any energy barrier and in presence of only a weak repulsive interaction potential or a monotonically decaying potential, particles do not have enough kinetic energy required to maintain their position in an aggregated state. Therefore, as soon as particles come into contact with each other, there will be no barrier left which will prevent their further association into clusters.

The absence of any energy barriers as observed in Tables 8 - 11 suggests that the aggregate formation in Model-2 takes place in **diffusion-limited regime**, whereby the main process determining the collision between particles is the Brownian motion. The enhancement in hydrophobic interactions results in reduction in the magnitude of repulsive interactions but no attractive well or secondary barrier to hinder aggregation is formed.

5.2 Stability Analysis

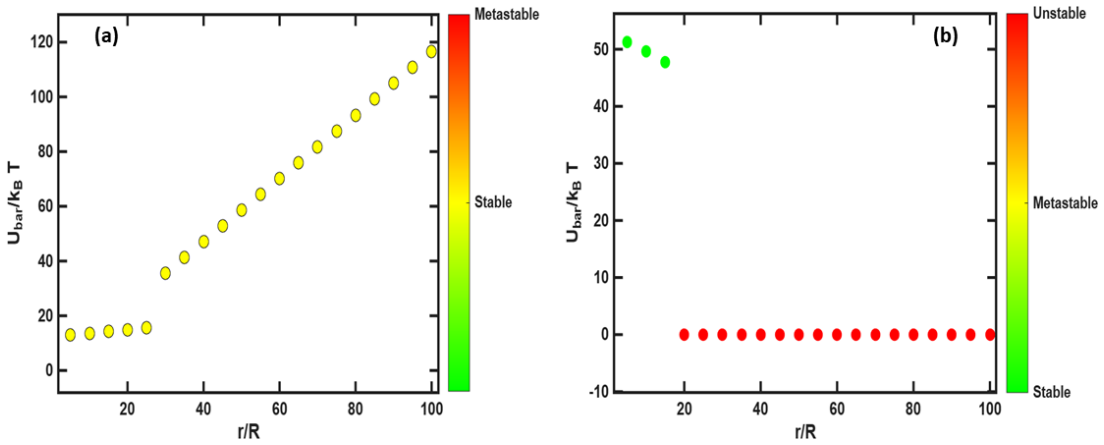

Fig. 12 Stability regime classification based on energy barrier (a) Model-1 and (b) Model-2

According to Model-1, the inter-particle interaction is regulated via the hydrophobic attraction and the electrostatic repulsion with the presence of an energy barrier, which determines the kinetic stability against clustering. Given a constant hydrophobic fraction h_f = 10%, the stability regime for all examined particle sizes can be justified with sufficiently high energy barriers indicated in Table 12.

The increase in particle size results in an increasing depth of the first minimum and increasing energy barrier height U_{bar}. The latter grows from around 13 k_BT (for a = 5 nm) to 110 k_BT (at a = 100 nm) for the particles (see Table 12). Such dependence of the energy barrier height as a function of the particle size, illustrated in Fig. 12 (a), shows that the larger particle sizes provide better protection against aggregation.

Moreover, the scaling behavior reveals the linear increase in barrier and maximum forces for all investigated particle sizes, which can be seen from Fig. 13. Thus, the scaling behavior demonstrates that in Model-1, the geometrical scaling predominates over interaction range modification. However, although changing the Debye screening

parameter leads to the barrier variation, its dependence on the particle size remains linear (Fig. 13).

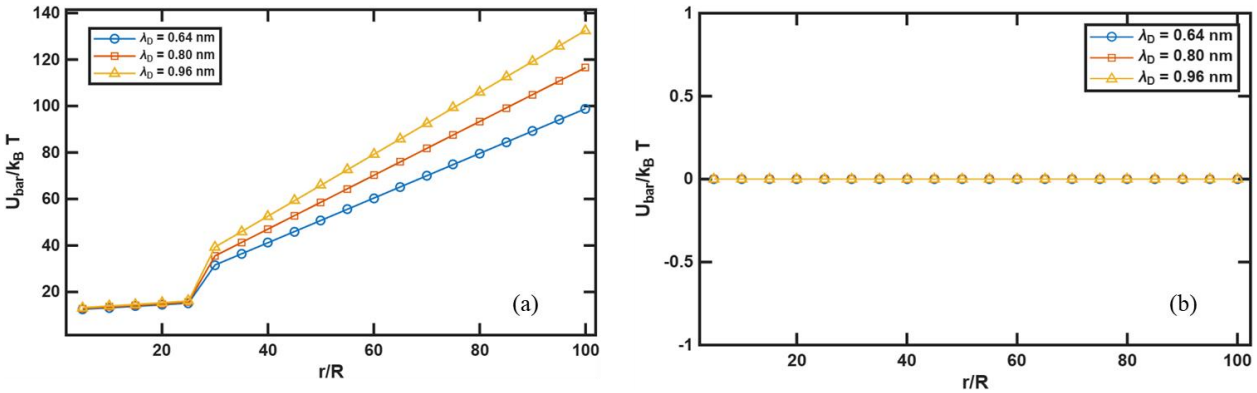

Fig. 13 Energy Barrier Sensitivity to Debye Length (a) Model-1 and (b) Model-2.

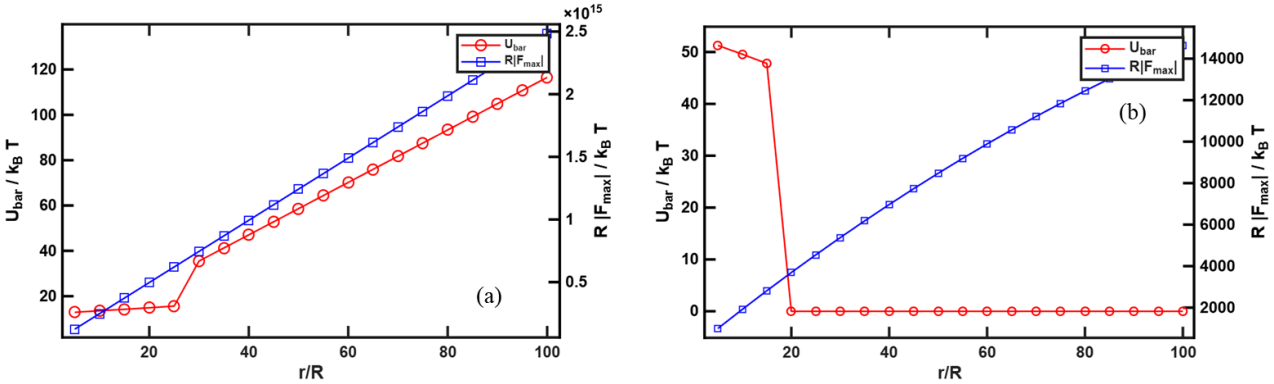

Fig. 14 Dimensionless scaling of energy barrier and Interaction force (a) Model-1 and (b) Model-2.

The effect of interactions between particles in Model-2 involves repulsion from the surfaces, which gives rise to different behavior in comparison to that of Model-1. For a particular hydrophobic fraction value of h_f = 10%, the energy barriers are stable only in cases where the size of particles does not exceed a value of 15 nm, whereas for higher particle sizes, the energy barrier does not exist at all. As shown in Fig. 12(b) and confirmed by the Table 12, the system predominantly falls into the **unstable regime** for most particle sizes.

Scaling analysis shows that while there is a linear increase in the maximum interaction force with increasing particle size, the energy barrier falls down to zero after the critical particle size (see Fig. 14(b)). This means that particle size does not play an important role in kinetic stabilization in Model-2. In addition, changing the value of Debye

screening length will not give rise to an energy barrier. The barrier height will always be equal to zero for any screening length (Fig. 13(b)).

Absence of energy barrier means that the collision of the particles does not require any special energetic conditions and hence occurs diffusively without any reversibility. After collision, the particles approach each other; however, there is no energy barrier that prevents the interaction between particles. This causes unstable aggregation in Model-2.

Table 12: Size-dependent interaction energy, force, and stability regimes in Model-1 (h_f = 10%).

R (nm)	Primary min (k_BT)	Barrier (k_BT)	Stability Regime
5	-14.446	12.982	1
10	-26.581	13.656	1
15	-39.114	18.444	1
20	-51.752	24.146	1
25	-64.433	29.888	1
30	-77.135	35.651	1
35	-89.851	41.426	1
40	-102.58	47.208	1
45	-115.3	52.995	1
50	-128.04	58.786	1
55	-140.78	64.58	1
60	-153.52	70.376	1
65	-166.26	76.174	1
70	179	81.974	1
75	-191.74	87.775	1
80	-204.49	93.577	1
85	-217.24	99.381	1
90	-229.99	105.18	1
95	-242.73	110.99	1
100	-255.48	116.8	1

Table 13: Size-dependent interaction energy, force, and stability regimes in Model-2 (h_f = 10%).

R (nm)	Primary min (k_BT)	Barrier (k_BT)	Stability Regime
5	-36.498	51.264	1
10	-22.998	49.57	1
15	-9.4983	47.792	1
20	0.84564	0	3
25	1.0571	0	3
30	1.2685	0	3
35	1.4799	0	3
40	1.6913	0	3
45	1.9027	0	3
50	2.1141	0	3
55	2.3255	0	3
60	2.5369	0	3
65	2.7483	0	3
70	2.9597	0	3
75	3.17121	0	3
80	3.3826	0	3
85	3.594	0	3
90	3.8054	0	3
95	4.0168	0	3
100	4.2282	0	3

5.3 Particle Size Effects on Interaction Forces

The effect of variation of particle size on the magnitude of the maximum interaction force is not the same for the two models. In the case of Model-1, an increase in particle size causes an increase in the maximum force in a linear fashion (Fig. 15(a)). This enhanced force scale contributes to the formation of large energy barriers, thereby suppressing particle aggregation and promoting kinetic stability.

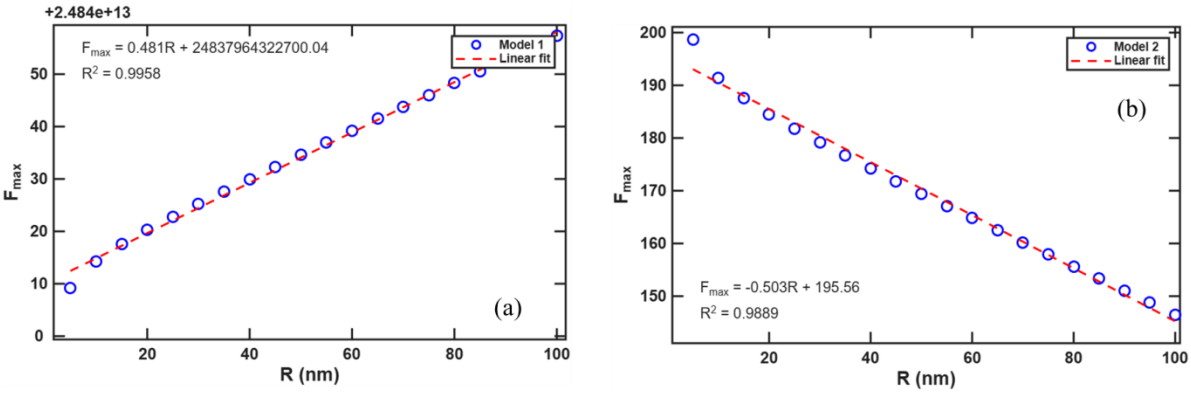

Fig. 15 Maximum interaction force Fmax as a function of particle size R for (a) Model-1 and (b) Model-2 systems at a constant hydrophobic fraction, i.e., hf = 10%. Notice the reversal of the slope on changing the non-DLVO component of the interaction. See text for details.

In contrast, Model-2 exhibits a linear decrease in the maximum interaction force with increasing particle size (Fig. 15(b)). Despite the presence of measurable interaction forces, the absence of a corresponding energy barrier prevents kinetic stabilization. Consequently, particle encounters are not hindered energetically, leading to diffusion-limited and irreversible aggregation in Model-2.

Chapter – 6

AGGREGATION OF ELASTIN

Elastin is a hydrophobic fibrous protein found in the vertebrate tissues including major blood vessels, lungs, and skin. This biopolymer is associated with high shear elastic modulus that enables reversible stretching and recoiling. Such outstanding mechanical properties owe their origin to the regular arrangement of hydrophobic domains of non-polar amino acids like glycine, alanine, valine, and leucine and lysine in its molecular structure. Tropoelastin is the monomeric precursor for elastin, which is insoluble, non-glycosylated, and highly hydrophobic, and it undergoes self-aggregation, and phase separation following a complex thermodynamic process which is temperature dependent [3,28]. The aggregation behavior of this physiologically important hydrophobic protein was extensively studied in ethanolic solvent by Pawar et al [3]. It was found that at above a threshold temperature ~ 297 K there was a propensity of hydrophobic interactions that caused enhanced protein aggregation. This was modeled via an extended-DLVO model by incorporating a surface tension force as the non-DLVO component in the constitutive equation (Eq.1). It was concluded that the hydrophobic interactions between the protein molecules were overwhelmingly dominant over other interactions which caused instability due to enhanced aggregation, which leads to liquid-liquid phase separation, often called coacervation [28,29].

Let us apply the Model-2 interaction protocol to explain the aggregation behavior of elastin. This model stipulates that for small particles hydrophobic interaction dominates near contact, and unlike the molecular scale attraction this interaction doesn't change significantly with particle size until a limit. However, as size increases further electrostatic and contributions arising from surface-related forces become increasingly dominant, and the hydrophobic forces alone are inadequate to sustain a stabilizing barrier (primary minima). Consequently, a size-dependent crossover from attraction-dominated behavior at small size to an unstable interaction regime at larger size arises that may lead to a phase separation. In the elastin aggregation studies a similar growth of particle size dominated crossover from a stable one-phase dispersion (elastin solution) to a two-phase liquid-liquid phase separation was noticed, which was attributed to coacervation [29]. It is well known that coacervation is a thermodynamic phase transition triggered by strong associative interactions between polyelectrolytes

[30]. Thus, we notice a qualitative concurrence of our model with the aggregation behavior reported for the hydrophobic protein elastin.

Chapter – 7

AGGREGATION OF ZEIN

Zein is a class of prolamine protein (a group of plant proteins found with very high proline content) mostly found in maize. Zein is composed of large amount (> 50%) of hydrophobic amino acids, such as proline, glutamine, and asparagine, leucine and alanine, but low in the essential amino acids lysine and tryptophan. It is a storage protein and constitutes as much as half of the total protein of the endosperm. Zein has a helical wheel shaped structure with nine homologous units arranged in non-parallel with the units stabilized by hydrogen bonds. This helical shape gives zein a globular morphology. This water-insoluble, but alcohol-soluble corn storage protein is one of the poorly understood biomacromolecules as far as its aggregation properties under different solvent conditions are concerned.

It is reported that this hydrophobic plant protein forms nanoparticles in ethanolic solutions with specific aggregation attributes [31]. Homogeneous aggregates of low size and polydispersity were formed close to its pI (~6.2). In contrast, in the presence of a monovalent salt, these particles exhibited aggressive heterogeneous aggregation with the formation of large aggregates of high polydispersity [31]. Zein which contains large amounts of non-polar and hydrophobic amino acids aggregates readily following significantly different self-organization pathways in a dominant manifestation of interplay of various interactions in the milieu of a binary solvent. Here too, we may apply the implications of Model-2 to understand the aggregation kinetics of zein. It was noticed that maximum aggregation occurred at the isoelectric pH (pI) of zein which is 6.2. Thus, there was a propensity of aggregation when the net charge on the protein was marginal. In such a scenario the dominant contributions associative interactions would arise from the hydrophobic and surface forces. The particle size growth profile revealed a biphasic pattern with an initial sharp increase in aggregate size followed by a slower growth. In the absence of an electrical double layer, the hydrophobic attractive forces were dominant until a size of about two times the size of the original (monomer) was achieved. Beyond that there was a smooth cross-over led by surface forces that provoked aggregation albeit slowly, and large clusters emerged consistent with the predictions of Model-2.

Chapter – 8

CONCLUSIONS

This work investigates the phenomenon of protein/colloid aggregation via an extended version of the DLVO approach emphasizing hydrophobic interaction. A scaling relation was established between the interaction force and particle/biomolecular size which explicitly depends on the surface property. Model-1 focused on the attractive potential at the molecular-scale where the resulting interaction showed the presence of kinetically stabilized aggregation states. However, such models, which are suitable for conventional colloidal systems, may not always be realistic, especially considering the environment in which biomolecular systems resides. In contrast, Model 2, which emphasized the hydrophobic force showed barrier less interaction with deep primary minima. This result pertains to systems that follow diffusion-limited aggregation like hydrophobic proteins. Furthermore, it shows that smaller particles demonstrate DLVO-like behavior, whereas for systems with higher hydrophobic potentials form larger aggregates aggressively due to the absence of any energy barrier. Finally, it is necessary to comment on the experimental validation of the results obtained. Clearly, this requires hydrophobicity-dependent size data for proteins in a given system over a wide range, for which there is a paucity of data. Regardless, an attempt has been made to qualitatively discuss the aggregation behavior of two hydrophobic proteins, elastin and zein, within the ambit of one of the interaction models proposed in this work.

Chapter – 9

FUTURE WORK

Future work may extend the present DLVO-based framework by incorporating additional interaction potentials beyond hydrophobicity. While the current study focuses on hydrophobic interactions as the dominant non-DLVO contribution, similar analyses can be performed by introducing other non-DLVO forces such as steric, depletion, hydration, or specific binding interactions. A further exploration of these effects in conjunction with an expanded DLVO theory will enable one to gain more insight into the force balance involved in determining protein stability.

From another perspective, an integration of the above theories with experiments is a critical issue to consider in future studies. A microfluidic approach that can investigate hydrophobic aggregation at a precisely defined ionic strength and controllable shear environment is one potential area of research.

10. LIST OF COMMUNICATED/ACCEPTED CONFERENCE PUBLICATION(S) & JOURNAL PUBLICATIONS

The paper has been selected for two Oral Presentations.

1. <u>International Conference on Recent Advances in Nanoscience and Nanotechnology (ICRANN – 2025)</u>

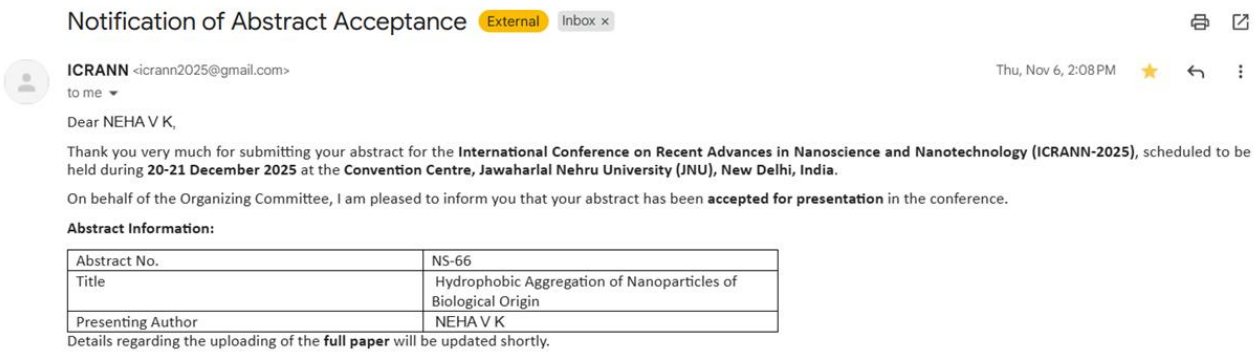

Notification of Abstract Acceptance External Inbox ×

ICRANN <icrann2025@gmail.com> Thu, Nov 6, 2:08 PM

to me

Dear NEHA V K,

Thank you very much for submitting your abstract for the **International Conference on Recent Advances in Nanoscience and Nanotechnology (ICRANN-2025)**, scheduled to be held during **20-21 December 2025** at the **Convention Centre, Jawaharlal Nehru University (JNU), New Delhi, India**.

On behalf of the Organizing Committee, I am pleased to inform you that your abstract has been **accepted for presentation** in the conference.

Abstract Information:

Abstract No.	NS-66
Title	Hydrophobic Aggregation of Nanoparticles of Biological Origin
Presenting Author	NEHA V K

Details regarding the uploading of the **full paper** will be updated shortly.

2. <u>International Conference on Atomic, Moelcular, Nano and Optical Physics with Applications (IAMNOP – 2025)</u>

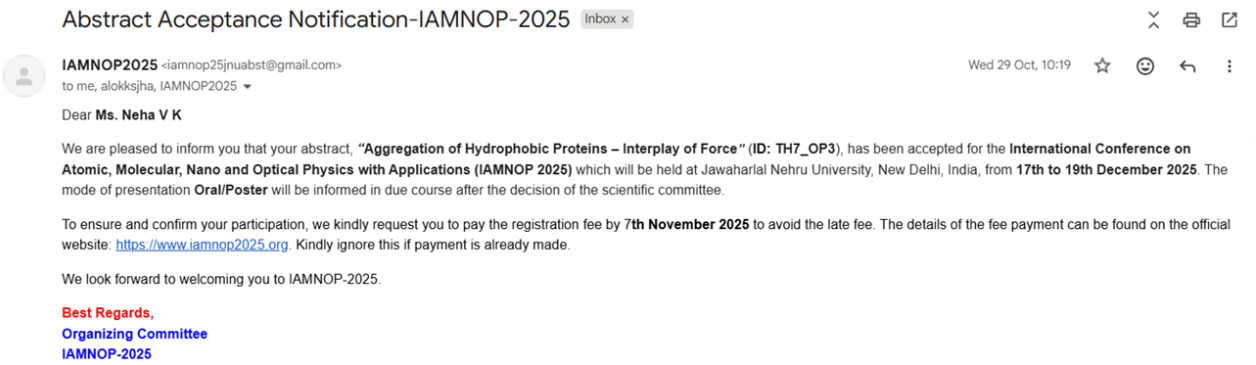

Abstract Acceptance Notification-IAMNOP-2025 Inbox ×

IAMNOP2025 <iamnop25jnuabst@gmail.com> Wed 29 Oct, 10:19

to me, alokksjha, IAMNOP2025

Dear **Ms. Neha V K**

We are pleased to inform you that your abstract, **"Aggregation of Hydrophobic Proteins – Interplay of Force" (ID: TH7_OP3)**, has been accepted for the **International Conference on Atomic, Molecular, Nano and Optical Physics with Applications (IAMNOP 2025)** which will be held at Jawaharlal Nehru University, New Delhi, India, from **17th to 19th December 2025**. The mode of presentation **Oral/Poster** will be informed in due course after the decision of the scientific committee.

To ensure and confirm your participation, we kindly request you to pay the registration fee by 7**th November 2025** to avoid the late fee. The details of the fee payment can be found on the official website: https://www.iamnop2025.org. Kindly ignore this if payment is already made.

We look forward to welcoming you to IAMNOP-2025.

Best Regards,
Organizing Committee
IAMNOP-2025

3. <u>Colloid and Polymer Science.</u>

Manuscript has been submitted and is under the processing.

REFERENCES

[1] G. Hummer, S. Garde, A.E. García, M.E. Paulaitis, L.R. Pratt, Hydrophobic effects on a molecular scale, J. Phys. Chem. B 102 (1998) 10469–10482.

[2] H.B. Bohidar, Fundamentals of polymer physics and molecular biophysics, Cambridge University Press, Cambridge, UK, 2015.

[3] N. Pawar, P. Kaushik, H.B. Bohidar, Hydrophobic hydration and anomalous diffusion of elastin in an ethanolic solution, Phys. Chem. Chem. Phys. 19 (2017) 13994–14000.

[4] Y.-H. Lin, J. Song, J.D. Forman-Kay, H.S. Chan, Random-phase-approximation theory for sequence-dependent, biologically functional liquid-liquid phase separation of intrinsically disordered proteins, J. Mol. Liq. 228 (2017) 176–193.

[5] W. Pulawski, U. Ghoshdastider, V. Andrisano, S. Filipek, Ubiquitous amyloids, Appl. Biochem. Biotechnol. 166 (2012) 1626–1643.

[6] V. Norris, J. Oláh, S. Krylov, V. Uversky, J. Ovadi, The Sherpa hypothesis: Phenotype-protecting disordered proteins stabilize the phenotypes of neurons and oligodendrocytes, Research Square [preprint] (2023).

[7] A. Stradner, P. Schurtenberger, Potential and limits of a colloid approach to protein solutions, Soft Matter 16 (2020) 307–323.

[8] V. Agmo Hernández, An overview of surface forces and the DLVO theory, ChemTexts 9 (2023) 10.

[9] D. Horinek, DLVO theory, in: G. Kreysa, K. Ota, R. F. Savinell (Eds.), Encyclopedia of Applied Electrochemistry, Springer, New York, 2014, pp. 343–346.

[10] S. Stoll, J. Buffle, Computer simulations of colloids and macromolecules aggregate formation: Kolumne, CHIMIA 49 (1995) 300.

[11] I. Mela, E. Aumaitre, A.-M. Williamson, G.E. Yakubov, Charge reversal by salt-induced aggregation in aqueous lactoferrin solutions, Colloids Surf. B Biointerfaces 78 (2010) 53–60.

[12] L. Li, R. Zhang, Y. Guo, J. Ge, S. Lan, F. Tian, Y.-T. Long, H. You, J. Fang, Updated insights into the mechanism of salt-induced aggregation-based single-molecule surface-enhanced Raman spectroscopy, Adv. Sci. 12 (2025) 2417025.

[13] S. Pusara, P. Yamin, W. Wenzel, M. Krstić, M. Kozlowska, A coarse-grained xDLVO model for colloidal protein–protein interactions, Phys. Chem. Chem. Phys. 23 (2021) 12780–12794.

[14] S. Goswami, J. Bajpai, A.K. Bajpai, Designing gelatin nanocarriers as a swellable system for controlled release of insulin: An in-vitro kinetic study, J. Macromol. Sci. Part A 47 (2019) 119–130.

[15] J.A. Cedano, E. Querol, A. Mozo-Villarías, How hydrophobicity shapes the architecture of protein assemblies, Eur. Phys. J. E 46 (2023) 62.

[16] H.-J. Schneider, Distinction and quantification of noncovalent dispersive and hydrophobic effects, Molecules 29 (2024) 1591.

[17] T.-C. Lim, The relationship between Lennard-Jones (12-6) and Morse potential functions, Z. Naturforsch. A 58 (2003) 615–617.

[18] A. Vijaykumar, T.E. Ouldridge, P.R. ten Wolde, P.G. Bolhuis, Multiscale simulations of anisotropic particles combining molecular dynamics and Green's function reaction dynamics, J. Chem. Phys. 146 (2017) 114106.

[19] J.M. Prausnitz, Molecular thermodynamics for some applications in biotechnology, J. Chem. Thermodyn. 35 (2003) 21–39.

[20] M.A. Blanco, E. Sahin, A.S. Robinson, C.J. Roberts, Coarse-grained model for colloidal protein interactions, B_{22}, and protein cluster formation, J. Phys. Chem. B 117 (2013) 16013–16028.

[21] S. Lower, Hydrogen-bonding and water, Chem1 Virtual Textbook, Simon Fraser University. http://www.chem1.com/acad/webtext/virtualtextbook.html, 2023.

[22] G. Pellicane, D. Costa, C. Caccamo, Theory and simulation of short-range models of globular protein solutions, J. Phys. Condens. Matter 16 (2004) S4923–S4936.

[23] E. Mani, W. Lechner, W.K. Kegel, P.G. Bolhuis, Equilibrium and non-equilibrium cluster phases in colloids with competing interactions, Soft Matter 10 (2014) 4479–4486.

[24] V. Bianco, G. Franzese, Hydrogen bond correlated percolation in a supercooled water monolayer as a hallmark of the critical region, J. Mol. Liq. 285 (2019) 727–739.

[25] J.G. Kirkwood, On the theory of strong electrolyte solutions, J. Chem. Phys. 2 (1934) 767–781.

[26] P. Varilly, A.P. Willard, J.B. Kirkegaard, T.P.J. Knowles, D. Chandler, Intra-chain organisation of hydrophobic residues controls inter-chain aggregation rates of amphiphilic polymers, J. Chem. Phys. 146 (2017) 135102.

[27] S. Auer, A. Trovato, M. Vendruscolo, A condensation-ordering mechanism in nanoparticle-catalyzed peptide aggregation, PLoS Comput. Biol. 5 (2009) e1000458.

[28] L.D. Muiznieks, S. Sharpe, R. Pomès, F.W. Keeley, Role of liquid–liquid phase separation in assembly of elastin and other extracellular matrix proteins, J. Mol. Biol. 430 (2018) 4741–4753.

[29] P. Kaushik, K. Rawat, H.B. Bohidar, Heat-induced coacervation of elastin and its possible thermoreversibility, Colloid Polym. Sci. 297 (2019) 947–956.

[30] C.E. Sing, S.L. Perry, Recent progress in the science of complex coacervation, Soft Matter 16 (2020) 2885–2914.

[31] A. Mallik, A study on protein aggregation, M.Sc. thesis, School of Physical Science, Jawaharlal Nehru University, New Delhi, India, 2019.

DELHI TECHNOLOGICAL UNIVERSITY

(Formerly Delhi College of Engineering)

Shahbad Daulatpur, Main Bawana Road, Delhi-110042

PLAGIARISM VERIFICATION REPORT

Title of the Thesis	: Hydrophobic Aggregation of Colloids and Proteins: Size Dependent Behavior and Crossover to Instability
Total Pages	: 54
Name of the Student	: Neha V K
Supervisor	: Prof. Himadri B. Bohidar Honorary Faculty Department of Applied Physics

This is to certify that the above thesis was examined using Turnitin plagiarism detection software and the similarity analysis report is summarized below.

Software used	: Turnitin
Similarity Index	: 6%
AI Similarity	: 0%
Total Word Count	: 7716

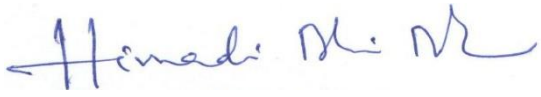

Candidate's Signature **Signature of Supervisor(s)**

Date: 28 May 2026

PLAGIARISM REPORT

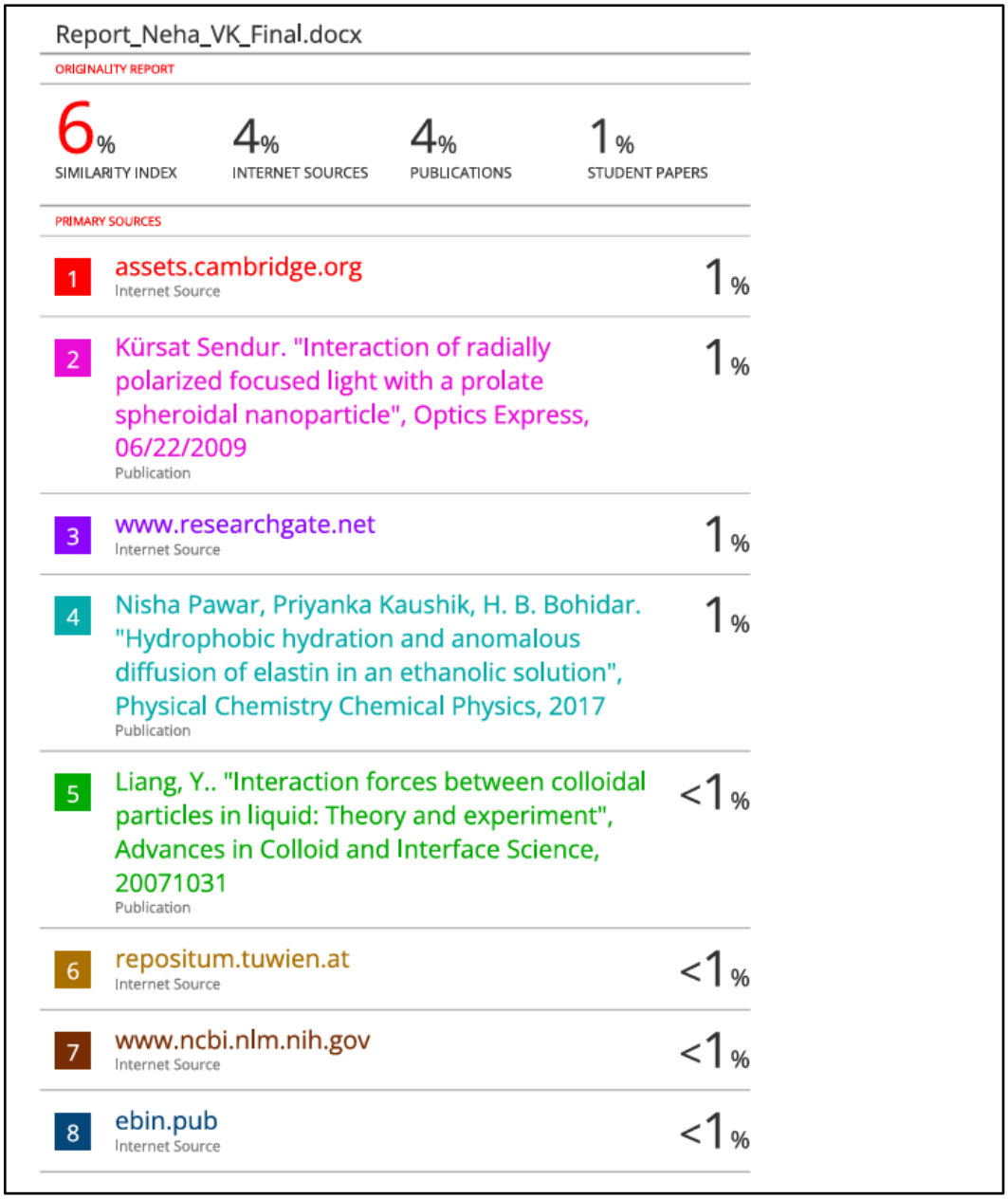

Report_Neha_VK_Final.docx

ORIGINALITY REPORT

6%	4%	4%	1%
SIMILARITY INDEX	INTERNET SOURCES	PUBLICATIONS	STUDENT PAPERS

PRIMARY SOURCES

1	assets.cambridge.org Internet Source	1%
2	Kürsat Sendur. "Interaction of radially polarized focused light with a prolate spheroidal nanoparticle", Optics Express, 06/22/2009 Publication	1%
3	www.researchgate.net Internet Source	1%
4	Nisha Pawar, Priyanka Kaushik, H. B. Bohidar. "Hydrophobic hydration and anomalous diffusion of elastin in an ethanolic solution", Physical Chemistry Chemical Physics, 2017 Publication	1%
5	Liang, Y.. "Interaction forces between colloidal particles in liquid: Theory and experiment", Advances in Colloid and Interface Science, 20071031 Publication	<1%
6	repositum.tuwien.at Internet Source	<1%
7	www.ncbi.nlm.nih.gov Internet Source	<1%
8	ebin.pub Internet Source	<1%

9	S. Watanabe, M. Taki, T. Tanaka, Y. Watanabe. "FDTD analysis of microwave hearing effect", IEEE Transactions on Microwave Theory and Techniques, 2000 Publication	<1 %
10	old.dpg-tagungen.de Internet Source	<1 %
11	www.ogtr.gov.au Internet Source	<1 %
12	Dan Geraghty, Mark A. Peifer, Irwin Rubenstein, Joachim Messing. "The primary structure of a plant storage protein: zein", Nucleic Acids Research, 1981 Publication	<1 %
13	Submitted to Swinburne University of Technology Student Paper	<1 %
14	Submitted to University of Lancaster Student Paper	<1 %
15	lcpe.uni-sofia.bg Internet Source	<1 %
16	Brett K. Brunk. "Hydrodynamic pair diffusion in isotropic random velocity fields with application to turbulent coagulation", Physics of Fluids, 1997 Publication	<1 %
17	Kianoush, M.R.. "Effect of vertical acceleration on response of concrete rectangular liquid storage tanks", Engineering Structures, 200604 Publication	<1 %
18	core.ac.uk Internet Source	<1 %

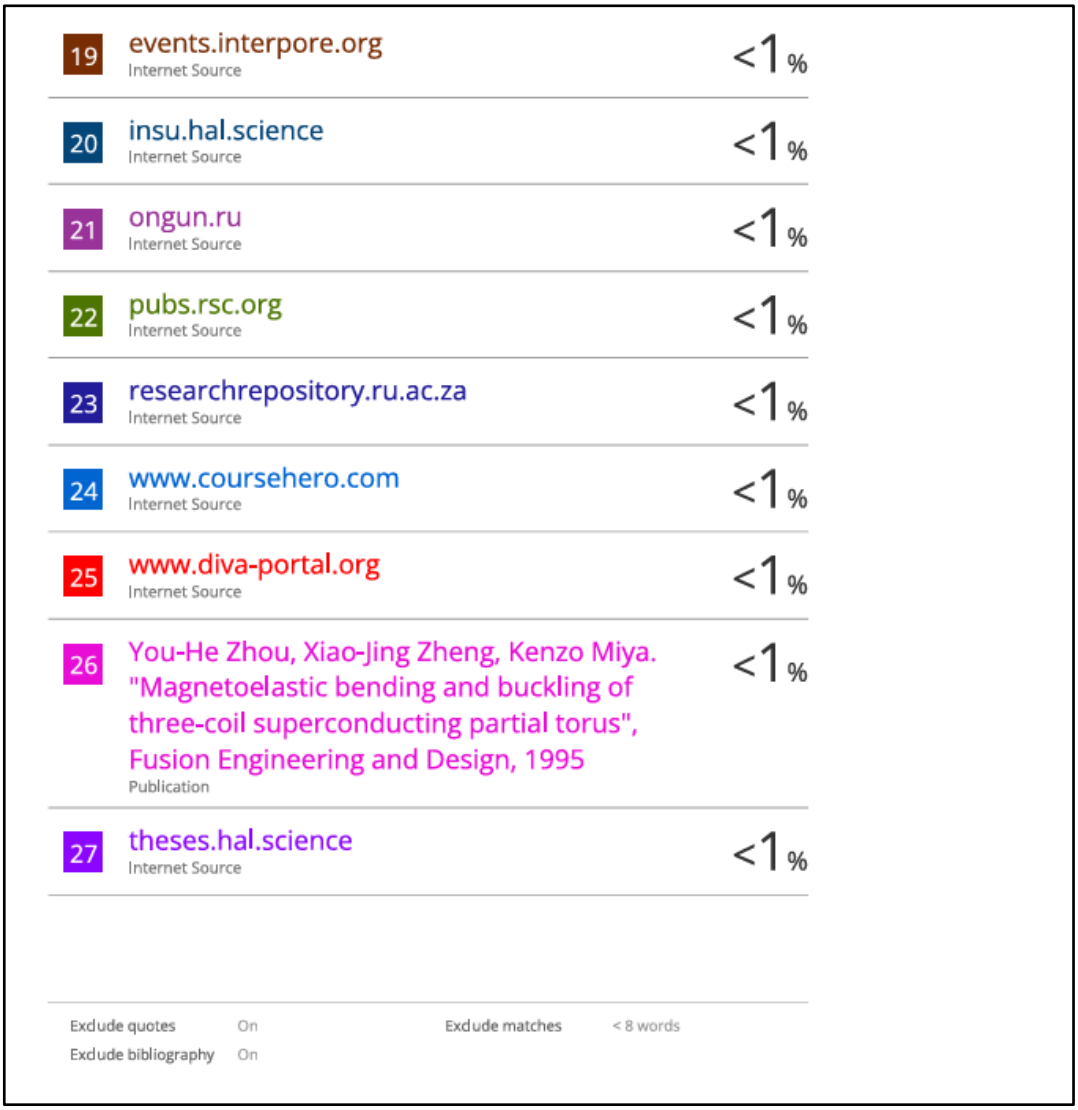
19 events.interpore.org
Internet Source
<1%
20 insu.hal.science
Internet Source
<1%
21 ongun.ru
Internet Source
<1%
22 pubs.rsc.org
Internet Source
<1%
23 researchrepository.ru.ac.za
Internet Source
<1%
24 www.coursehero.com
Internet Source
<1%
25 www.diva-portal.org
Internet Source
<1%
26 You-He Zhou, Xiao-Jing Zheng, Kenzo Miya. "Magnetoelastic bending and buckling of three-coil superconducting partial torus", Fusion Engineering and Design, 1995
Publication
<1%
27 theses.hal.science
Internet Source
<1%
Exclude quotes On
Exclude bibliography On
Exclude matches < 8 words

AI SIMILARITY REPORT

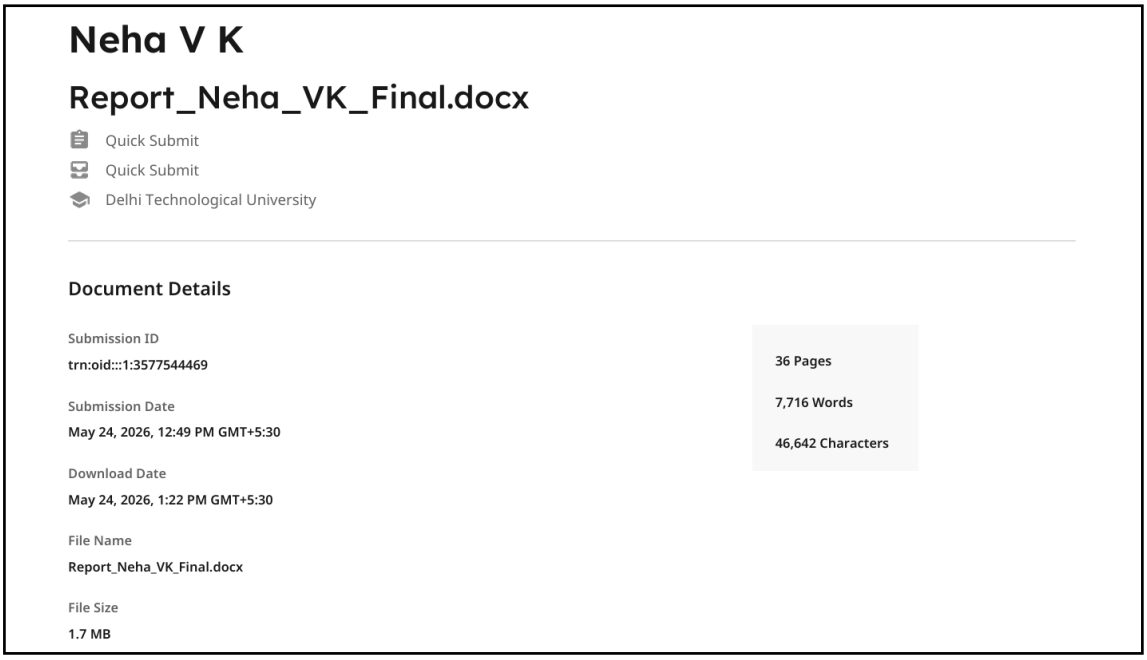

Neha V K

Report_Neha_VK_Final.docx

Quick Submit

Quick Submit

Delhi Technological University

Document Details

Submission ID
trn:oid:::1:3577544469

Submission Date
May 24, 2026, 12:49 PM GMT+5:30

Download Date
May 24, 2026, 1:22 PM GMT+5:30

File Name
Report_Neha_VK_Final.docx

File Size
1.7 MB

36 Pages

7,716 Words

46,642 Characters

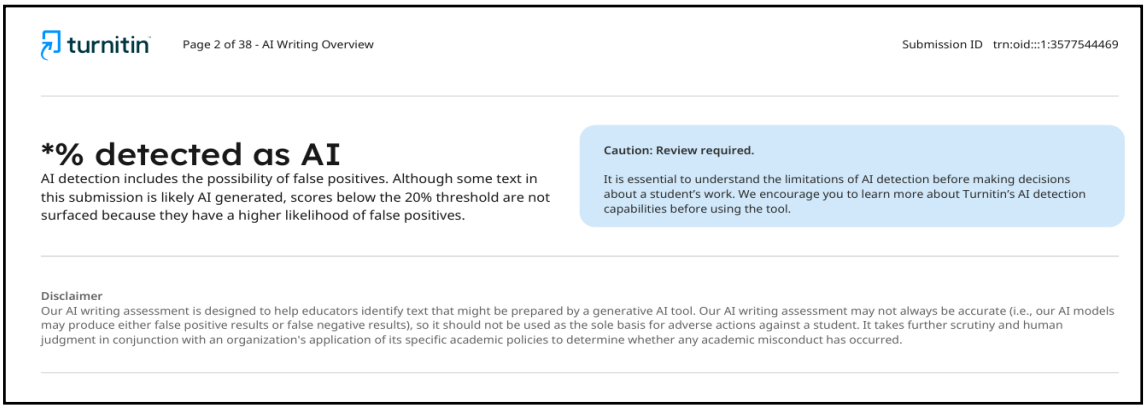

turnitin Page 2 of 38 - AI Writing Overview Submission ID trn:oid:::1:3577544469

*% detected as AI

AI detection includes the possibility of false positives. Although some text in this submission is likely AI generated, scores below the 20% threshold are not surfaced because they have a higher likelihood of false positives.

Caution: Review required.

It is essential to understand the limitations of AI detection before making decisions about a student's work. We encourage you to learn more about Turnitin's AI detection capabilities before using the tool.

Disclaimer
Our AI writing assessment is designed to help educators identify text that might be prepared by a generative AI tool. Our AI writing assessment may not always be accurate (i.e., our AI models may produce either false positive results or false negative results), so it should not be used as the sole basis for adverse actions against a student. It takes further scrutiny and human judgment in conjunction with an organization's application of its specific academic policies to determine whether any academic misconduct has occurred.

APPENDIX I

CONFERENCE CERTIFICATE

Certificate of Participation

This certificate is presented to

Neha VK

Title: Hydrophobic aggregation of nanoparticles of biological origin

In recognition of oral presentation in

3rd International Conference on Recent Advances in Nanoscience and Nanotechnology-2025 (ICRANN-2025)

Organized by: Special Centre for Nanoscience, Jawaharlal Nehru University, New Delhi -110067, India. December 20–21, 2025

Prof. Bijoy Kumar Kuanr
Chair, ICRANN-2025
JNU, New Delhi

APPENDIX II

JOURNAL PAPER – COLLOID AND POLYMER SCIENCE

Aggregation of Hydrophobic Colloids and Proteins: Size Dependent Behavior and Crossover to Instability

Neha V.K. and Himadri B. Bohidar*

Department of Applied Physics, Delhi Technological University

Bawana Road, Delhi-110042

Corresponding author email: bohidarjnu@gmail.com; hbbohidar@jnu.ac.in

ABSTRACT

This work focuses on the aggregation properties of hydrophobic colloids within the framework of modified DLVO theory where an additional short-range interaction is introduced. Two different interaction models are examined to investigate the specific role of hydrophobic interaction in particle aggregation kinetics. Model I considers van der Waals attraction, electrostatic double layer repulsion, as well as the surface effects which give rise to interaction forces with finite energy barriers ensuring kinetic stabilization of dispersions for particles of various size ($5 < R < 100$ nm) having different surface hydrophobicity ($0 < h_f < 20$ %). Model II considers a regime of interaction between particles in terms of hydrophobic attraction described by an exponential potential that results in the disappearance of the energy barrier arising from Coulombic forces for larger particles leading to diffusion limited irreversible aggregation. Remarkably, the following universal power-law dependence of the maximum interaction force (F_{max}) with particle size (R) was established, $F_{max} \sim R^{\alpha}$, with $\alpha = \pm 0.5$ for Model I while for the second case (hydrophobicity regime) $\alpha = -0.5$, clearly indicating the absence of any energy barriers due to the predominance of the short-range interaction. Application of these concepts may be extended to study the aggregation of hydrophobic proteins presumed to be blobs.

Keywords: Hydrophobic colloidal aggregation, extended DLVO model, Interaction potential, size – dependent crossover, interaction force – particle size scaling.

APPENDIX III

PROOF OF SCIE INDEXING